

Electronic supplementary information (ESI)

Tryptophan-Glucosamine Conjugates Modulate Tau-Derived PHF6 aggregation at Low concentrations

Ashim Paul¹, Wen-Hao Li², Guru Krishnakumar Viswanathan¹, Elad Arad,³ Satabdee Mohapatra¹, Gao Li², Raz Jelinek,³ Ehud Gazit¹, Yan-Mei Li^{2,4,5}, and Daniel Segal^{1,6}*

¹School of Molecular Cell Biology & Biotechnology, Tel Aviv University, Tel Aviv 69978, Israel

²Department of Chemistry, Tsinghua University, Beijing 100084, China

³Department of Chemistry, Ben Gurion University of the Negev, Beer Sheva 84105, Israel

⁴Beijing Institute for Brain Disorders, Beijing 100069, China

⁵Center for Synthetic and Systems Biology, Tsinghua University, Beijing 100084, China

⁶Sagol Interdisciplinary School of Neurosciences, Tel Aviv University, Tel Aviv 69978, Israel

*** Correspondence:**

Prof. Daniel Segal

dsegal@post.tau.ac.il

Materials and Methods

Materials

Acetylated PHF6 peptide (Ac-VQIVYK-NH₂) was purchased from GL Biochem (Shanghai, China). Lipids were purchased from Avanti Polar Lipids (USA). D-Glucosamine Hydrochloride and Linkers (Fmoc- γ -Abu-OH, Fmoc-5-aminopentanoic acid, Fmoc-6-Ahx-OH) were purchased from Bide Pharmatech Ltd (Shanghai, China), Boc-Trp(Boc)-OH and HOBT (1-Hydroxybenzotriazole) were purchased from GL Biochem Ltd (Shanghai, China). EDC-HCl (1-Ethyl-3-(3-dimethylaminopropyl)carbodiimide hydrochloride), DIPEA (N,N-Diisopropylethylamine), Piperidine, and TFA (trifluoroacetic acid) were purchased from Innochem Co., Ltd. (Beijing, China). TIPS (Triisopropylsilane) was obtained from Tianjin Heowns Biochemical Technology Co., Ltd. (Tianjin, China). Methyl- α -D-glucopyranoside and L-Tryptophanamide hydrochloride were purchased from Alfa Aesar (Yehud, Israel). SH-SY5Y, neuroblastoma cell line was purchased from ATCC (ATCC® CRL-2266) (<https://www.atcc.org/products/all/CRL-2266.aspx>) and all the biological samples were obtained from Biological Industries (Israel) and experiments were performed at Tel Aviv University. All chemicals and reagents were of analytical grade. Unless otherwise stated, all chemicals were obtained from Sigma-Aldrich (Rehovot, Israel).

Synthetic protocol of the Amino Acid-Sugar conjugate molecules

In a 100 mL round bottom (RB) flask, 2.0 mmol (1 equiv) of linker molecule (For AS1, the linker was γ -Abu-OH; for AS2 the linker was 5-Aminopentanoic acid; and for AS3 the linker was 6-Ahx-OH) dissolved in 10 mL methanol in presence of DIPEA (710.0 μ L, 4.0 mmol, 2 equiv) was taken and stirred continuously under ice. Then, HOBT (405.1 mg, 3.0 mmol, 1.5 equiv.) and EDC-HCl (582.0 mg, 3 mmol, 1.5 equiv.) were added into the RB followed by addition of D-Glucosamine Hydrochloride (474.8 mg, 2.2 mmol, 1.1equiv.) dissolved in 8 mL of Methanol. The reaction mixture was stirred for 15 min under ice, followed by 14 h at room temperature.^{1,2} The reaction was monitored by TLC (eluent, DCM: Methanol=15:1). After that, 30 mL of distilled water were added into the RB and white precipitated appeared which was extracted by 25 mL of DCM for 3 times. The product was collected and dried under vacuum to get white solid powder, which was further treated with 10 mL of 20% piperidine/DMF for 1 h at room temperature to cleave the Fmoc group. The cleaved product (Product A, Scheme S1) was collected in cold ether as brown precipitate and dried under vacuum.

In a 100 mL RB, Boc-Trp(Boc)-OH (444.4 mg, 1.1 mmol, 1.1 equiv.) dissolved in 15 mL Methanol with DIPEA (710.0 μ L, 4 mmol, 4 equiv) was taken. Then, HOBT (202.5 mg, 1.5 mmol, 1.5 equiv) and EDC·HCl (291.0 mg, 1.5 mmol, 1.5 equiv) were added into the RB with constant stirring for 10 min under ice. Thereafter, product A (1 mmol, 1 equiv) dissolved in 10 mL was added into the reaction mixture and stirred for 15 min under ice followed by 14 h at room temperature. The reaction mixture was then concentrated and 50 mL cold ether were slowly added into the concentrated solution to get brown precipitate. The precipitate was filtered and first purified by column chromatography using DCM/Methanol (1:0, 20:1, 12:1) as eluent and further purified by alumina column using DCM/Methanol (4:1, 0:1) as eluent. The white purified powder was treated with TFA cocktail solution (95% TFA, 2.5% H₂O and 2.5% TIPS) for 2 h to cleave the Boc group. Then, the reaction mixture was concentrated and 50 mL of cold ether were slowly added into that to obtain white precipitate. The white precipitate was collected and purified by HPLC using H₂O/Acetonitrile as eluent on analytic C18 column. The analyzing gradient was 2% to 35% of solution B (80% acetonitrile/0.06% trifluoroacetic acid in water), with a flow rate of 0.8 mL/min. The solution A was prepared with double distilled water containing 0.06% trifluoroacetic acid. A dual UV detector (at λ_{max} 215 nm for amide bond and at λ_{max} 278 nm for Trp group) have been used to monitor the HPLC. Due to the unpreventable interconversion of 1-OH (α and β -isomers) of the AS molecules, there were two peaks observed in HPLC for each pure AS molecule while both were confirmed by ESI-MS.^{3,4} We named either of the isomer (e.g., α) as 1 and the other isomer (e.g., β) as 2, for instance AS1 as two isomers, AS1-1 and AS1-2. The purified products (AS, Scheme S1) were lyophilized to get white powder. The remaining two derivatives were prepared varying the linker following the same protocol mentioned above. ¹H-NMR and ¹³C-NMR were recorded in JNM-ECA400 and JNM-ECA600 instruments (Jeol, Japan). HRMS was performed in ESI IT-TOF Instrument Information: LCMS-IT/TOF (Shimadzu, Japan)

Characterization of the Amino Acid-Sugar based conjugates

1. **Amino acid sugar-based conjugate 1** (AS1, 4-((S)-2-amino-3-(1H-indol-3-yl)propanamido)-N-((3R,4R,5S,6R)-2,4,5-trihydroxy-6-(hydroxy methyl)tetrahydro-2H-pyran-3-yl)butanamide). Isolated Yield 35%. ¹H NMR (400 MHz, Methanol- d₄) δ 7.54 (d, J = 7.8 Hz, 1H), 7.29 (d, J = 8.0 Hz, 1H), 7.10 (s, 1H), 7.04 (t, J = 7.6 Hz, 1H), 6.98 (t, J = 7.5 Hz, 1H), 3.93 (t, J = 7.4 Hz, 1H), 3.69 (s, 5H), 3.50 (s, 1H), 3.18 – 2.99 (m, 4H), 2.00 (t, 2H), 1.65 – 1.50 (m, 2H). ¹³C NMR (150 MHz, Methanol- d₄) δ 175.63, 170.09, 138.26, 128.28, 125.49, 122.95, 120.31, 119.11, 112.66, 108.18, 92.60, 73.13, 72.54,

64.31, 62.79, 55.78, 55.29, 40.06, 34.07, 28.90, 26.26. Calculated mass for $C_{21}H_{31}N_4O_7$ is 451.2187 $[M+H]^+$ and 473.2007 $[M+Na]^+$, observed 451.2187 $[M+H]^+$ and 473.1989 $[M+Na]^+$.

2. Amino acid sugar-based conjugate 2 (AS2, 5-((S)-2-amino-3-(1H-indol-3-yl)propanamido)-N-((3R,4R,5S,6R)-2,4,5-trihydroxy-6-(hydroxymethyl)tetrahydro-2H-pyran-3-yl)pentanamide). Isolated Yield 38%. 1H NMR (400 MHz, Methanol- d_4) δ 7.52 (d, $J = 7.9$ Hz, 1H), 7.28 (d, $J = 8.2$ Hz, 1H), 7.09 (s, 1H), 7.04 (t, $J = 7.6$ Hz, 1H), 6.96 (t, $J = 7.4$ Hz, 1H), 3.93 (t, $J = 7.4$ Hz, 1H), 3.86 – 3.45 (m, 5H), 3.21 (s, 3H), 3.04 (s, 2H), 2.09 (t, $J = 6.9, 0.0$ Hz, 3H), 1.48 – 1.33 (m, 1H), 1.33 – 1.21 (m, 1H). ^{13}C NMR (150 MHz, Methanol- d_4) δ 176.21, 169.98, 138.26, 128.29, 125.49, 122.91, 120.26, 119.09, 112.65, 108.17, 92.61, 73.12, 72.57, 62.79, 58.64, 55.81, 55.30, 40.16, 36.22, 29.33, 28.94, 23.83. Calculated mass for $C_{22}H_{33}N_4O_7$ is 465.2344 $[M+H]^+$ and 487.2163 $[M+Na]^+$, observed 465.2347 $[M+H]^+$ and 487.2149 $[M+Na]^+$.

3. Amino acid sugar-based conjugate 3 (AS3, 6-((S)-2-amino-3-(1H-indol-3-yl)propanamido)-N-((3R,4R,5S,6R)-2,4,5-trihydroxy-6-(hydroxymethyl)tetrahydro-2H-pyran-3-yl)hexanamide). Isolated Yield 40%. 1H NMR (400 MHz, Deuterium Oxide) δ 7.62 (d, $J = 7.9$ Hz, 1H), 7.52 (d, $J = 7.4$ Hz, 1H), 7.28 (s, 1H), 7.25 (t, $J = 7.1$ Hz, 1H), 7.18 (t, $J = 7.6$ Hz, 1H), 4.09 (t, 1H), 3.99 – 3.55 (m, 5H), 3.38 (d, 4H), 3.10 (s, 1H), 2.17 (t, $J = 7.5$ Hz, 2H), 1.41 (dd, 2H), 1.09 (dd, 2H), 0.89 (dd, 2H). ^{13}C NMR (150 MHz, Methanol- d_4) δ 176.50, 169.93, 138.14, 128.33, 125.46, 122.83, 120.20, 119.12, 112.59, 108.16, 92.59, 73.08, 72.51, 62.74, 58.50, 55.76, 55.28, 40.44, 36.72, 29.56, 28.82, 27.18, 26.38. Calculated mass for $C_{23}H_{35}N_4O_7$ is 479.2500 $[M+H]^+$ and 501.2320 $[M+Na]^+$, observed 479.2533 $[M+H]^+$ and 501.2321 $[M+Na]^+$.

Stock preparation

PHF6 peptide was monomerized first by pre-treatment with HFIP for 10 min and the solvent was evaporated using a Speed Vac. The resulting thin film was dissolved in MOPS (20 mM, pH 7.2) buffer and sonicated for 5 min. Concentration was determined (calculated according to ϵ_{280} of $1490 M^{-1}cm^{-1}$) and adjusted to 1 mM concentration as a stock solution. Stock solutions of Thioflavin S (ThS, 2 mM in 20 mM MOPS), and Heparin (100 μ M in MOPS) were prepared. The stocks of the conjugate molecules (AS1-3, 1 mM) were prepared by dissolving them in double distilled water, separately. All the stock solutions were diluted with MOPS (20 mM, pH 7.2) according to the requirement.

Thioflavin S assay

For self-assembly experiments, stock solution was diluted in 100 μL wells in a 96-well black plate so that the final mixture contained 50 μM of the PHF6 peptide and 30 μM ThS in 20 mM MOPS. Immediately prior to the experiment, Heparin (final concentration 10 μM) was added to initiate peptide aggregation. For the inhibition assay, PHF6 was incubated in the presence, of various doses, or absence of the conjugate molecules. For fibril disassembly assays, PHF6 was first incubated alone to self-assemble to reach plateau in ThS assay. Then the conjugate molecules, at various doses, were added separately to designated wells, and the assay was further continued. Control wells were supplemented with the conjugates alone. The ThS assay of the conjugate molecules were also performed in similar as described for PHF6. Kinetic fluorescence data were collected at 25 $^{\circ}\text{C}$ in triplicate using Infinite M200 microplate reader (Tecan, Switzerland). Excitation and emission wavelengths of ThS were 440 and 490 nm, respectively.

Circular dichroism spectroscopy

To analyze the secondary structure of the PHF6 peptide in the absence or presence of the tested conjugates, 300 μL of the sample was taken in a cuvette (path length 1 mm) and CD spectra were then recorded on a Chirascan spectrometer between the range of 190-260 nm, and the background was subtracted from the CD spectra. Samples for CD, were prepared in similar manner as described for the ThS assay except the addition of ThS dye to the samples.

Transmission Electron Microscopy

Samples (10 μL) were placed for 2 min on 400-mesh copper grids covered with carbon-stabilized Formvar film (Electron Microscopy Sciences (EMS), Hatfield, PA). Excess fluid was removed, and the grids were negatively stained with 2% uranyl acetate solution (10 μL) for 2 min. Finally, excess fluid was removed, and the samples were viewed using a JEM-1400 TEM (JEOL), operated at 80 kV.

Large Unilamellar Vesicles (LUVs) preparation and Carboxyfluorescein entrapment

The vesicles were prepared as described earlier.^{5,6} Briefly, the LUVs were prepared using three different lipids, DMPC, Cholesterol and GM1 with 68:30:2 molar ratios in 20 mM MOPS buffer of pH 7.2. Lipids were taken in clean glass vessel and dissolved to make 2 mM stock solution in chloroform and methanol (2:1) and the solvents were evaporated under vacuum. The lipid films were hydrated with 500 μ L of carboxyfluorescein solution (100 μ M) in buffer solution and immediately vortexed vigorously for 30 min to emulsify the lipid mixtures. Then, lipid solution was dipped into the liquid nitrogen for instant cooling and after 2 min the frozen solution was dipped into water bath at 50-60 $^{\circ}$ C for thawing. These steps of freeze-thaw were repeated five times and the excess dye was removed by ultracentrifugation at 20000 rpm. The supernatant solution was discarded and the lipid pellet was re-hydrated with the buffer solution. This step was repeated two more times to make sure no additional dye remains and the final lipid pellet was collected followed by addition of 500 μ L of buffer solution and vortexed to obtain homogenous suspension of 1 mM of dye loaded LUVs. Then, different samples (PHF6 in the absence or presence of the conjugate molecules) were treated with the dye loaded LUVs and the leakage was measure by carboxyfluorescein fluorescence. The LUV leakage study was performed in triplicate on Infinite M200 microplate reader (Tecan, Switzerland). Excitation and emission wavelengths of the carboxyfluorescein dye were 492 and 517 nm, respectively. Triton X-100 was used for complete dye release from the LUVs, and its fluorescence value was considered as 100% dye leakage. The percentage of dye leakage by each sample was calculated according to following equation (S1),

$$\% \text{ Leakage} = \frac{(\text{observed fluorescence} - \text{initial fluorescence})}{(\text{total fluorescence} - \text{initial fluorescence})} \times 100 \% \quad (\text{S1})$$

Dynamic light scattering (DLS) measurements^{7,8}

DLS measurements were performed with the different peptide samples (oligomers and mature fibrils) on a Malvern nano zetasizer (Malvern, UK) using a laser source with $\lambda=633$ nm and a detector at a scattering angle of $\theta = 173$ degrees. PHF6 peptide (50 μ M) was incubated in a similar manner as described for the ThS assay, in the absence of ThS dye, for 10 min and 150 min to generate oligomers and mature fibrils, respectively and the hydrodynamic diameter of them was immediately examined by

DLS. Prior to the analysis, samples were filtered through 0.45 μm PVDF membrane. The samples were placed in a disposable cuvette and held at the corresponding temperature during the analysis. For each sample, the analyses were recorded three times with 11 sub-runs using the multimodal mode. The Z-average diameter was calculated from the correlation function using Malvern technology software.

Cell cytotoxicity

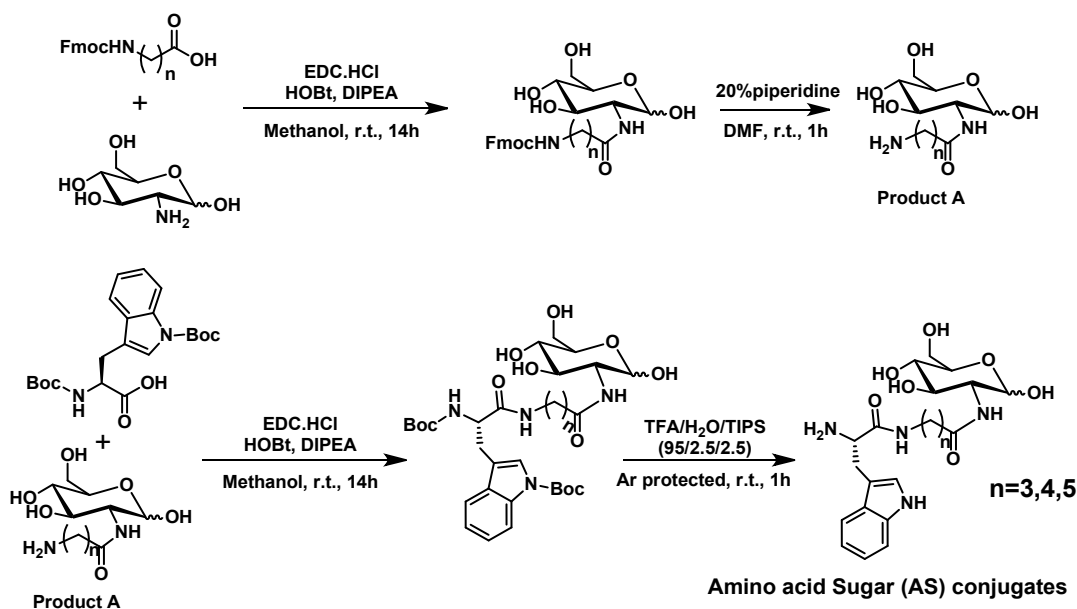
The SH-SY5Y cell line (2×10^5 cells/mL) was cultured in 96-well tissue microplates (100 μL /well) and allowed to adhere overnight at 37 $^\circ\text{C}$. The conjugate molecules were dissolved in DMEM:Nutrient mixture F12(Ham's) (1 :1) (Biological Industries, Israel) at different concentrations. The negative control, represented by zero, was prepared as medium without any conjugate molecules and treated in the same manner. 100 μL of medium with or without conjugates were added to each well. Following incubation for 24 h at 37 $^\circ\text{C}$, cell viability was evaluated using the 2,3-bis(2-methoxy-4-nitro-5-sulfophenyl)-2H-tetrazolium-5-carboxanilide (XTT) cell proliferation assay kit (Biological Industries, Israel) according to the manufacturer's instructions. Briefly, 100 μL of the activation reagent was added to 5 mL of the XTT reagent, followed by the addition of 100 μL of activated-XTT Solution to each well. After 2 h of incubation at 37 $^\circ\text{C}$, color intensity was measured using an ELISA microplate reader at 450 nm and 630 nm. Results are presented as mean and the standard error of the mean. Each experiment was repeated at least three times.

Isothermal Titration Calorimetry (ITC)

PHF6 was dissolved in MOPS buffer to 400 μM . AS1 solution (300 μL , 70 μM , dissolved in MOPS) was inserted into the Nano ITC low volume cell (TA Instruments, Newcastle, DE) and the titrating syringe was filled with 50 μL of PHF6 solution. The system reached stable temperature of 25 $^\circ\text{C}$. Then, PHF6 was titrated to the AS1 solution or MOPS buffer as control. The titration was carried out in 5 μL aliquots and let equilibrate for 300s before the next drop, along ten drops, of total 45 μL (the first drop is half volume). The resulted isotherm was analyzed using Nanoanalyze software using an independent interaction model. Baseline correction was performed by titrating AS1 to the MOPS blank.

Molecular Dynamics simulation

The co-ordinates of PHF6 peptides were obtained from PDB ID: 2ON9⁹ and the N-terminus of the peptide was acetylated. Further, the X-ray unit cell of the 2ON9 was replicated to attain the fibril structure consisting of 42 peptide units.⁶ Three-dimensional conformer of the conjugate AS1 was obtained as mentioned above and the GROMACS topology for the molecule was generated using the PRODRG Server. The atomic charge and charge groups of the ligands were generated based on the GROMOS96 54a7 force field parameters.¹⁰ AS1 molecules were placed inside the core of the fibril to elucidate its effect on PHF6 peptides. Control PHF6 fibril simulation was executed in the absence of AS1. Molecular dynamics simulation was performed in the isothermal-isobaric ensemble using GROMACS (4.5.3) with GROMOS96 54a7 force field, as described previously.^{5,6,10-12} Analyses of the trajectories were carried out using GROMACS suite of programs and PyMOL.



Scheme S1. A schematic representation for stepwise synthesis of Amino acid Sugar (AS) based conjugate molecules.

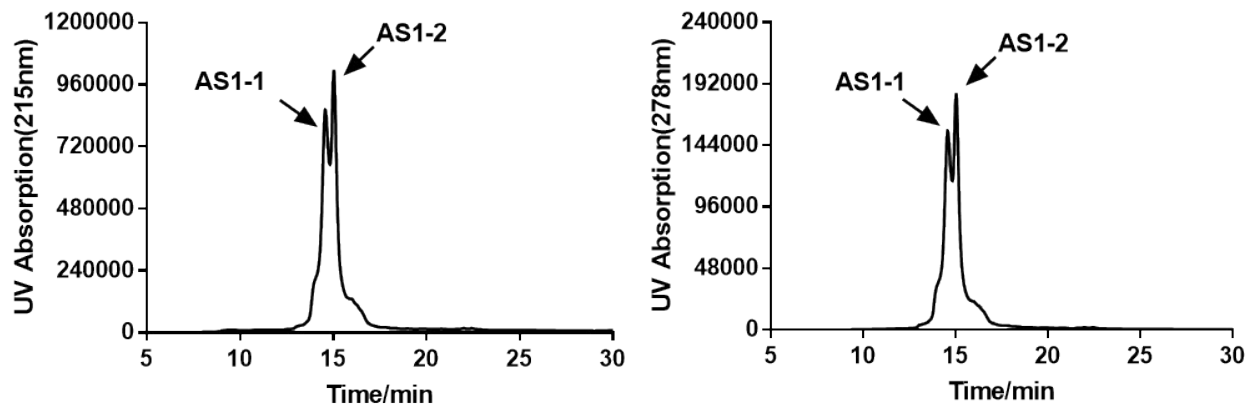


Figure S1. HPLC profile of AS1 (at $\lambda = 215$ nm, $\lambda = 278$ nm) with the retention time of 14.5 min (AS1-1) and 15.0 min (AS1-2).

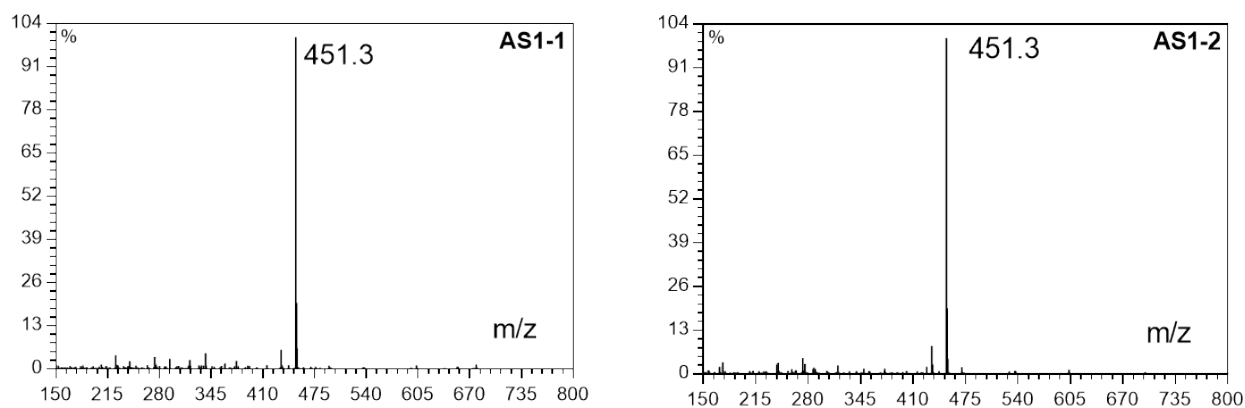


Figure S2. Mass spectrum of Compound AS1 (two isomers AS1-1 and AS1-2). Calculated mass for $C_{21}H_{31}N_4O_7$ is 451.2 $[M+H]^+$, observed 451.3 $[M+H]^+$.

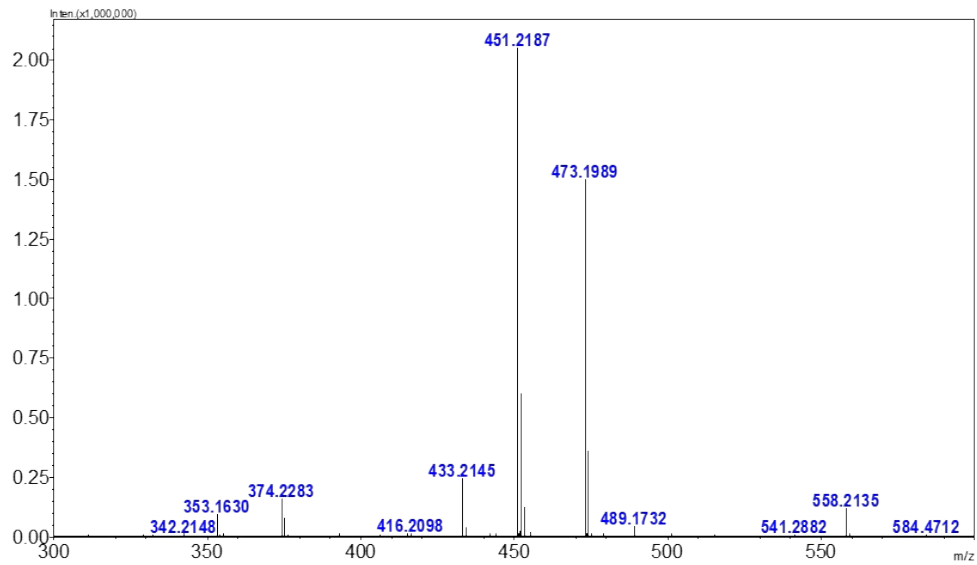


Figure S3. HRMS (ESI IT-TOF) mass spectrum of conjugate AS1. Calculated mass for $C_{21}H_{31}N_4O_7$ is 451.2187 $[M+H]^+$ and 473.2007 $[M+Na]^+$, observed 451.2187 $[M+H]^+$ and 473.1989 $[M+Na]^+$.

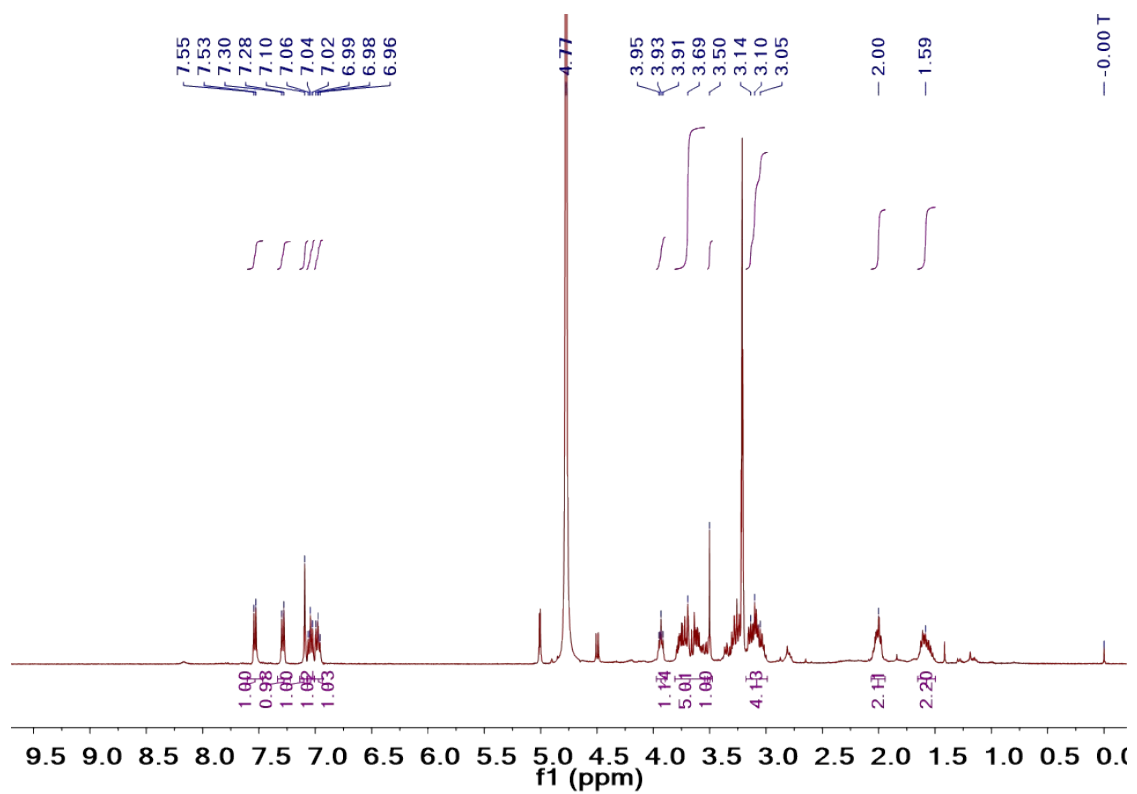


Figure S4. 1H NMR spectrum of conjugate AS1.

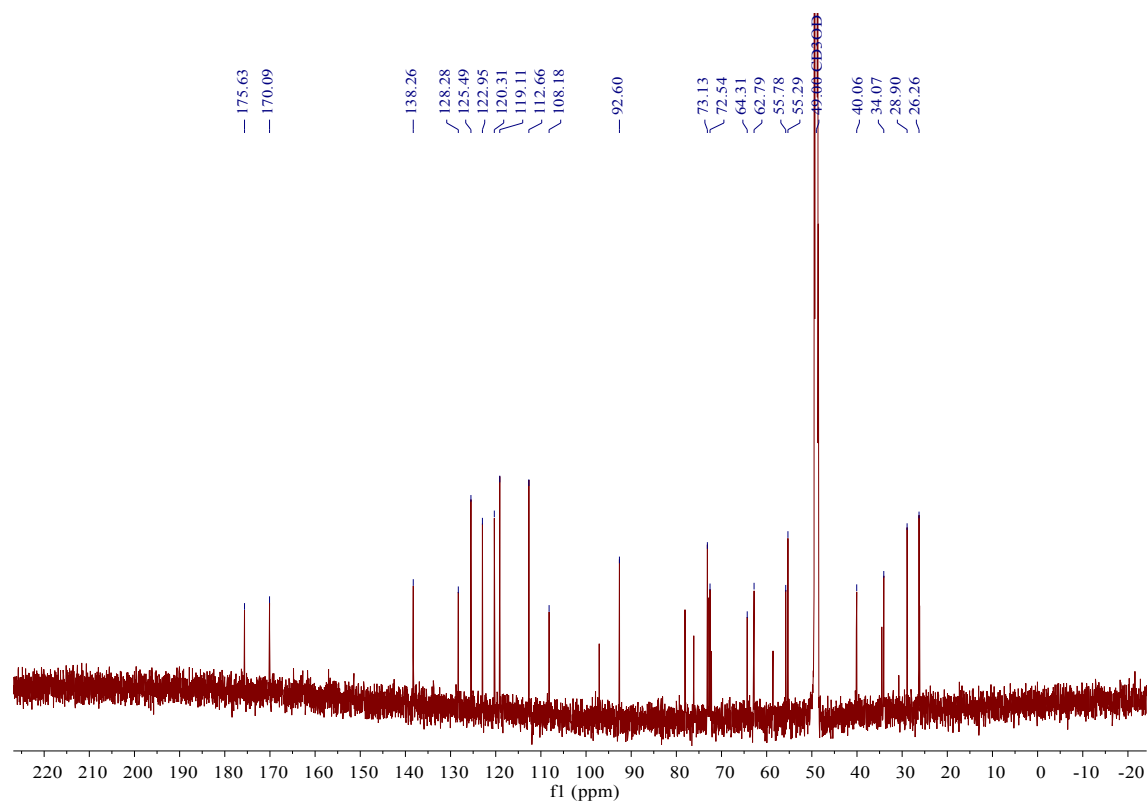


Figure S5. ^{13}C NMR spectrum of conjugate AS1.

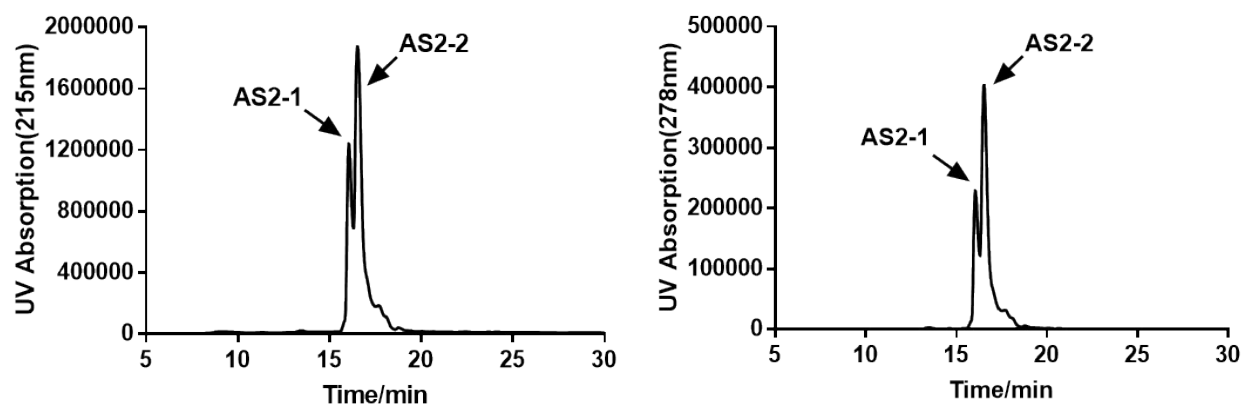


Figure S6. HPLC profile of AS2 (at $\lambda = 215$ nm, $\lambda = 278$ nm) with the retention time of 16.0 min (AS2-1) and 16.5 min (AS2-2).

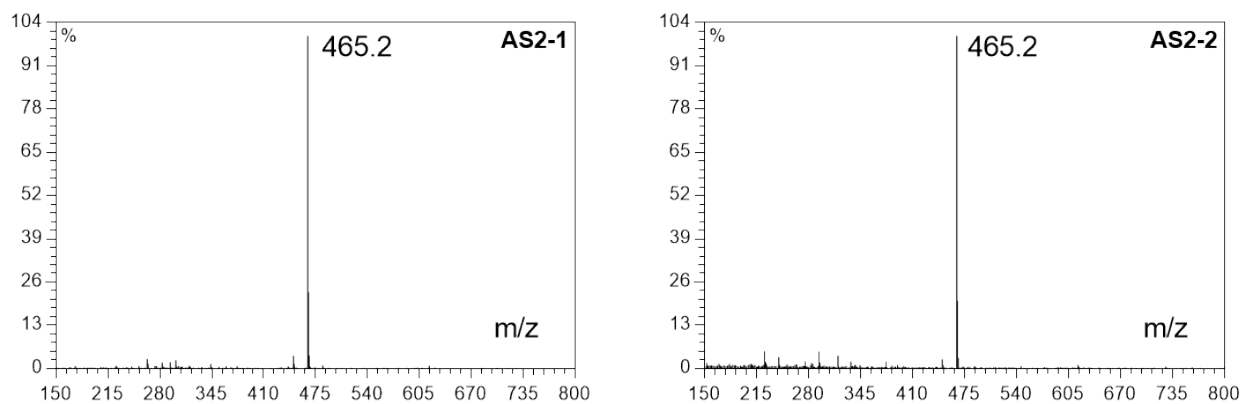


Figure S7. Mass spectrum of conjugate AS2 (two isomers AS2-1 and AS2-2). Calculated mass for $C_{22}H_{33}N_4O_7$ is 465.2 $[M+H]^+$, observed 465.2 $[M+H]^+$.

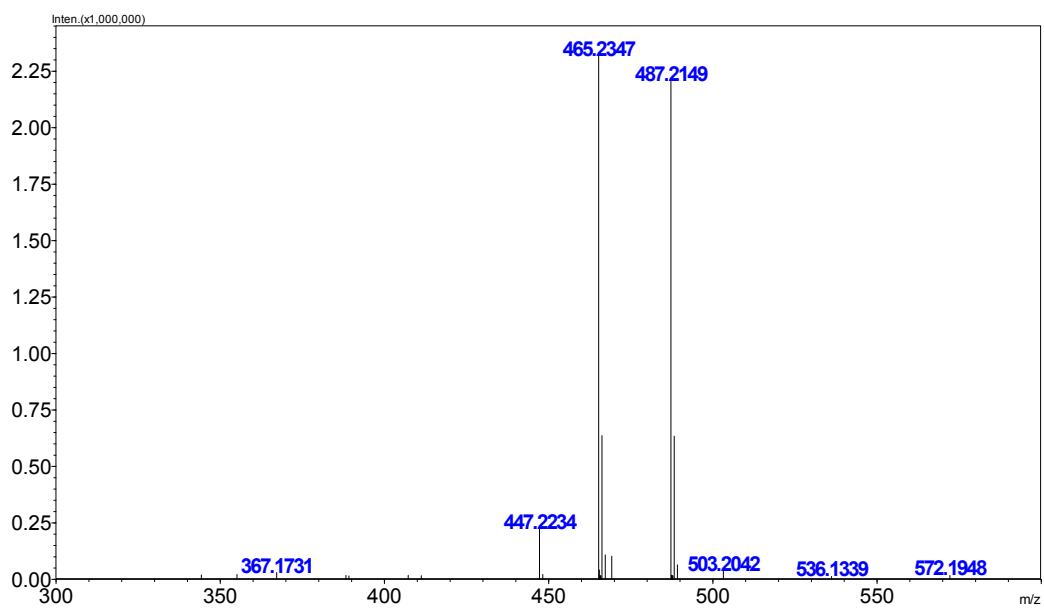


Figure S8. HRMS (ESI IT-TOF) mass spectrum of conjugate AS2. Calculated mass for $C_{22}H_{33}N_4O_7$ is 465.2344 $[M+H]^+$ and 487.2163 $[M+Na]^+$, observed 465.2347 $[M+H]^+$ and 487.2149 $[M+Na]^+$.

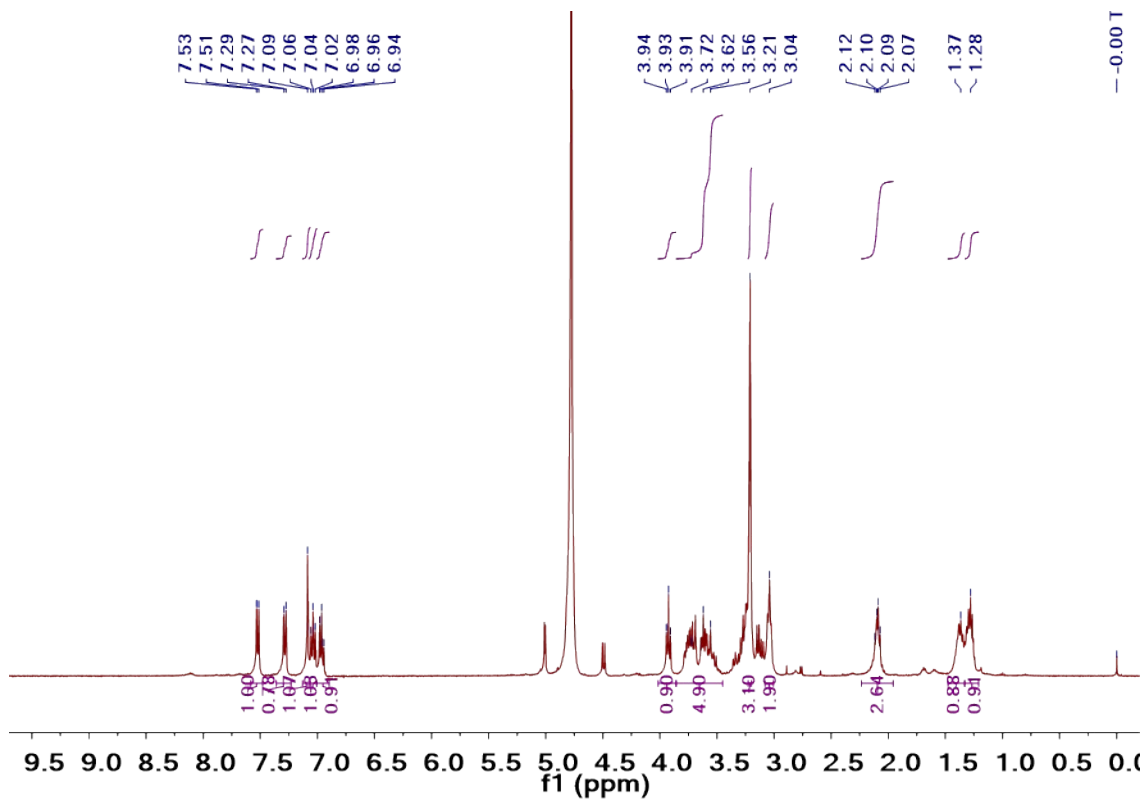


Figure S9. ^1H NMR spectrum of conjugate AS2.

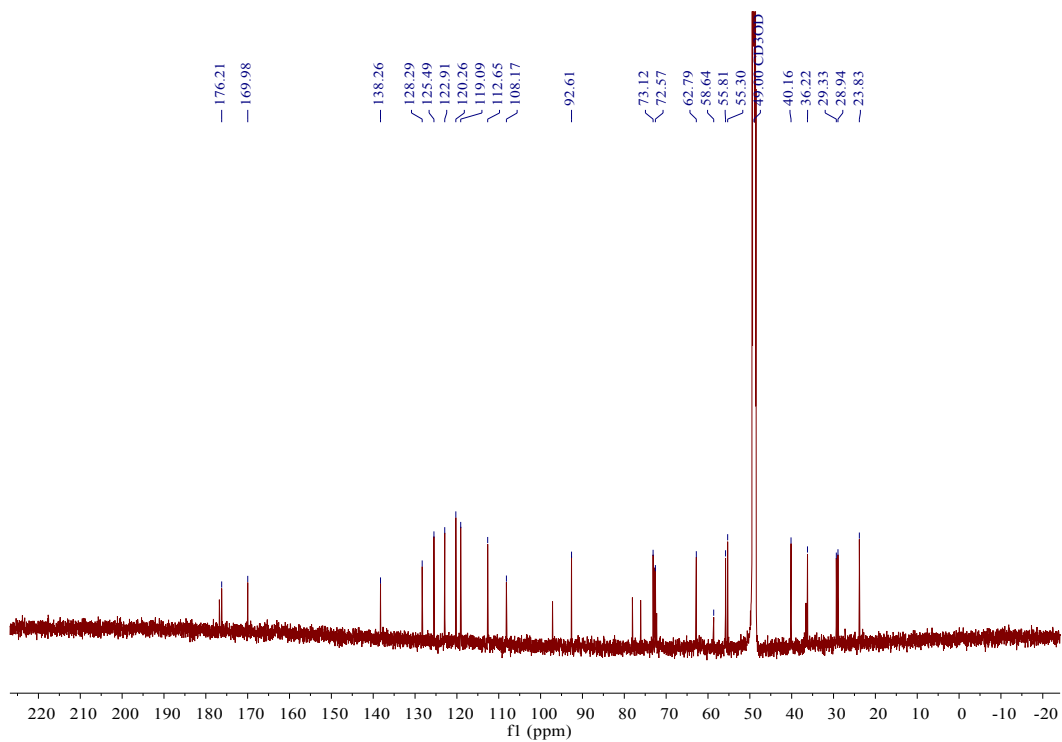


Figure S10. ^{13}C NMR spectrum of conjugate AS2.

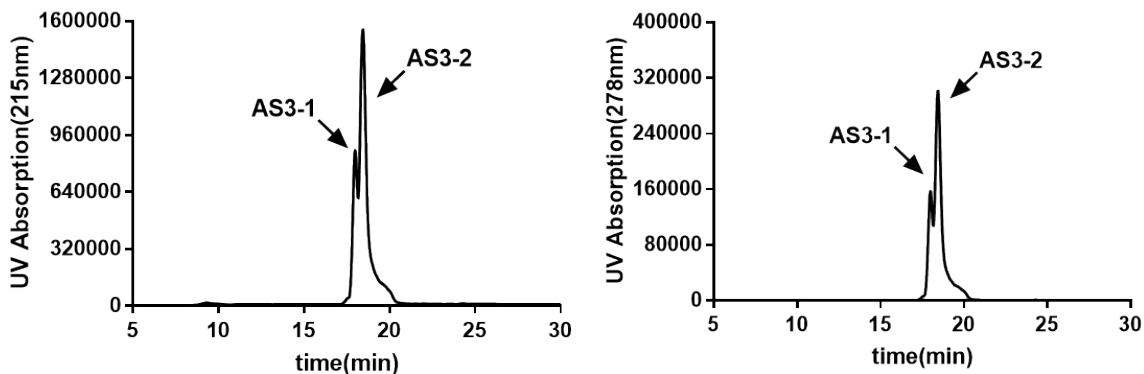


Figure S11. HPLC profile of AS3 (at $\lambda = 215$ nm, $\lambda = 278$ nm) with the retention time of 17.9 min (AS3-1) and 18.4 min (AS3-2).

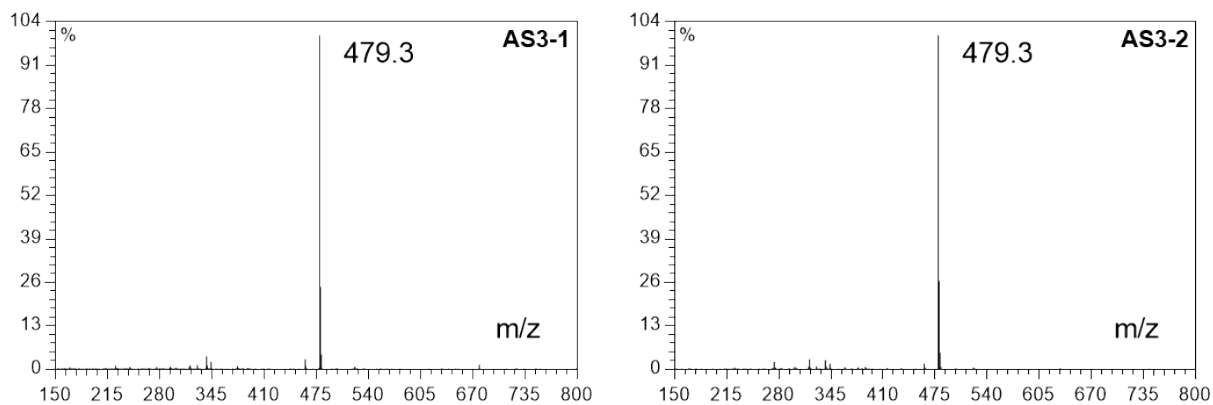


Figure S12. Mass spectrum of conjugate AS3 (two isomers AS3-1 and AS3-2). Calculated mass for $C_{23}H_{35}N_4O_7$ is 479.2 $[M+H]^+$, observed 479.3 $[M+H]^+$.

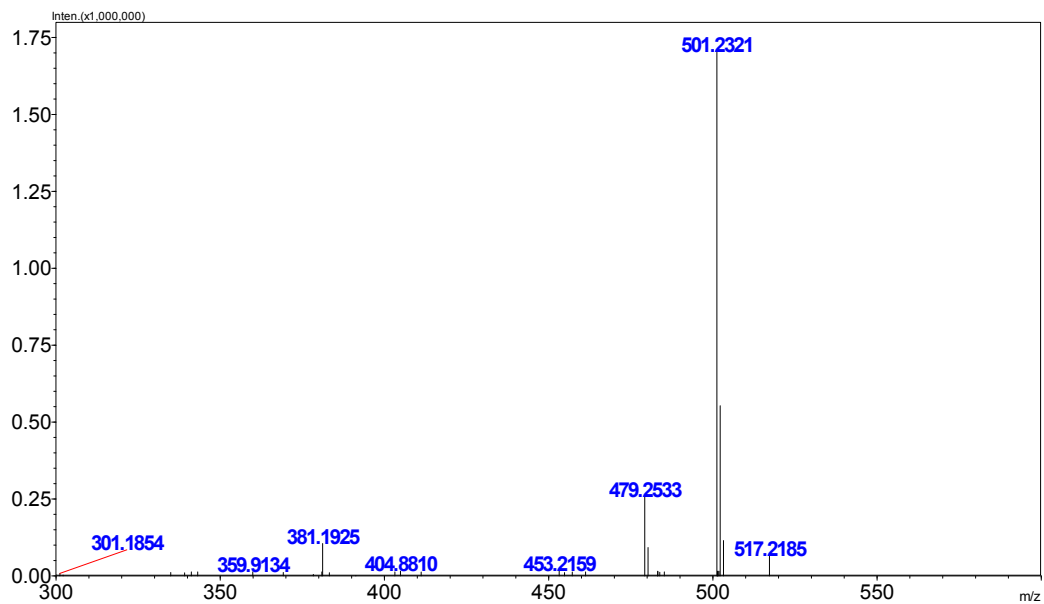


Figure S13. HRMS (ESI IT-TOF) mass spectrum of conjugate AS3. Calculated mass for $C_{23}H_{35}N_4O_7$ is 479.2500 $[M+H]^+$ and 501.2320 $[M+Na]^+$, observed 479.2533 $[M+H]^+$ and 501.2321 $[M+Na]^+$.

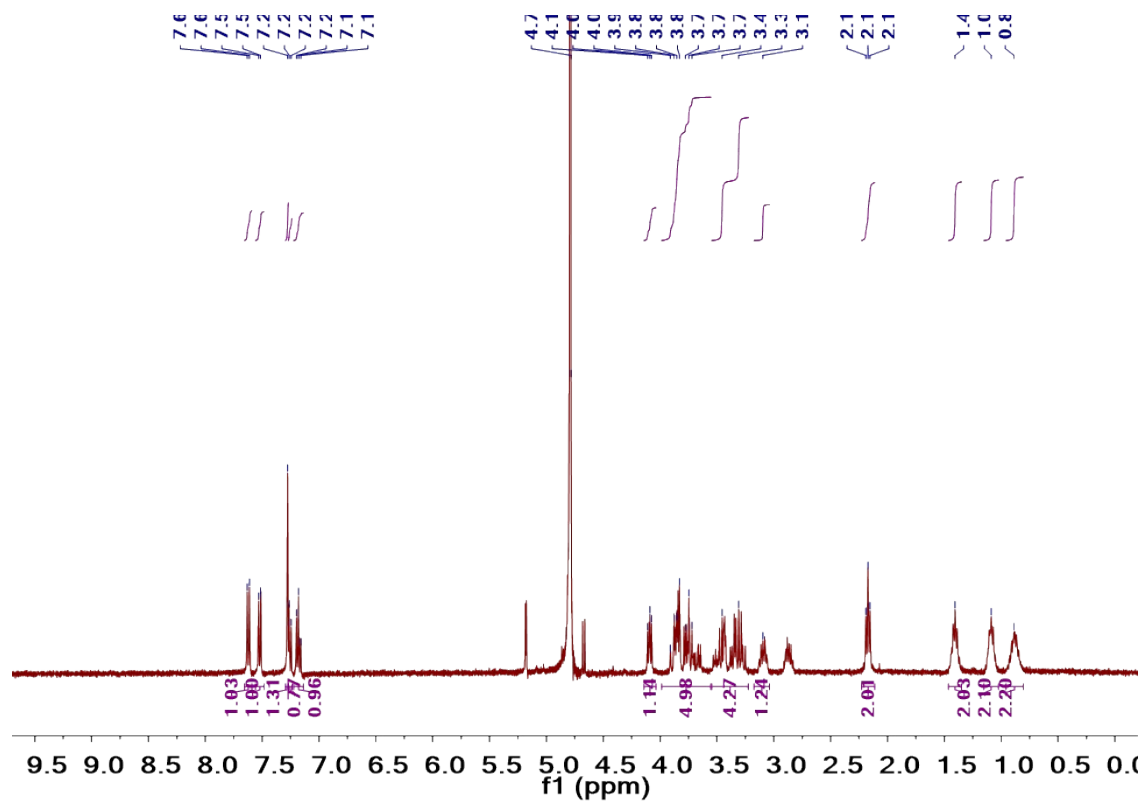


Figure S14. ^1H NMR spectrum of conjugate AS3.

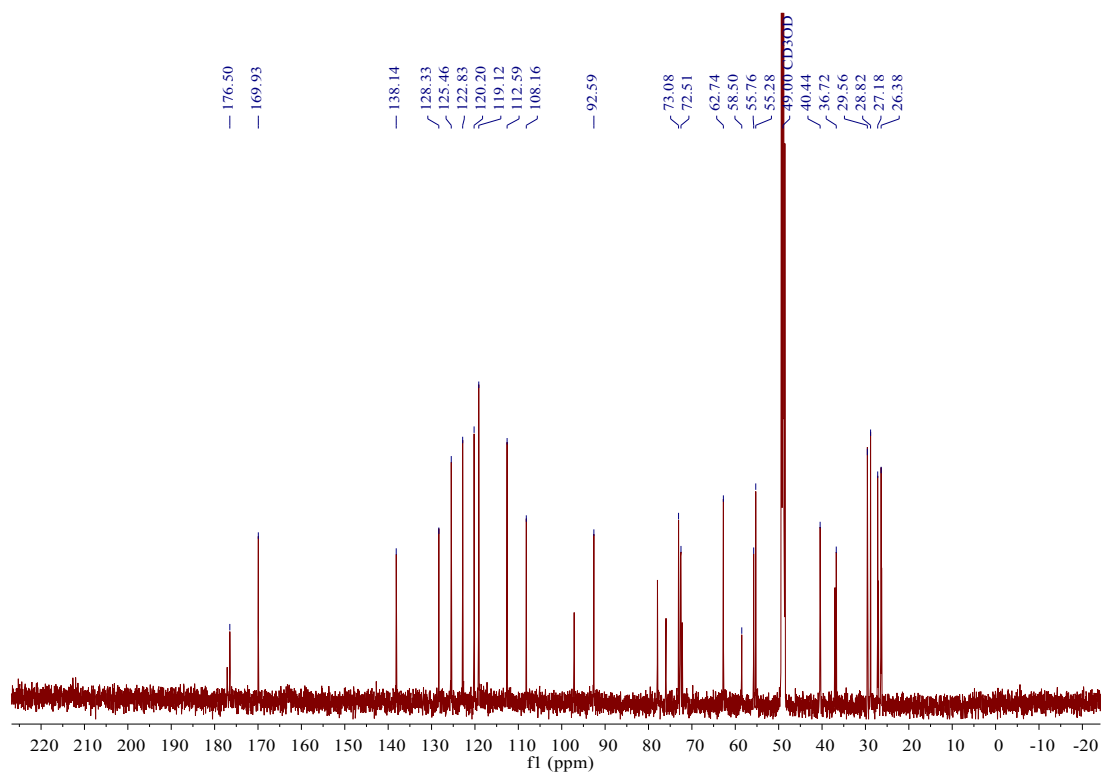


Figure S15. ^{13}C NMR spectrum of conjugate AS3.

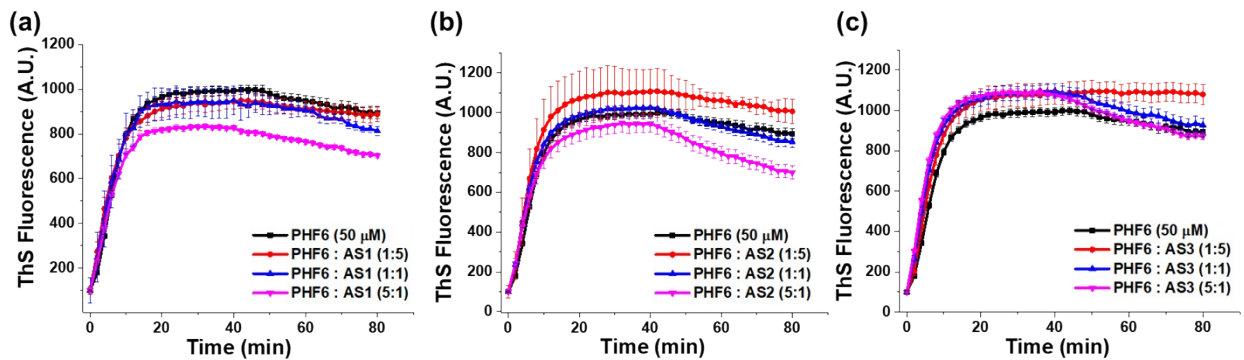


Figure S16. Time dependent ThS fluorescence of PHF6 aggregation ($50 \mu\text{M}$) in the absence or presence of various doses (PHF6 : conjugate- 1:0, 1:5, 1:1 and 5:1) of (a) AS1, (b) AS2 and (c) AS3. Experiments were performed in MOPS (pH 7.2, 20 mM) at 25°C .

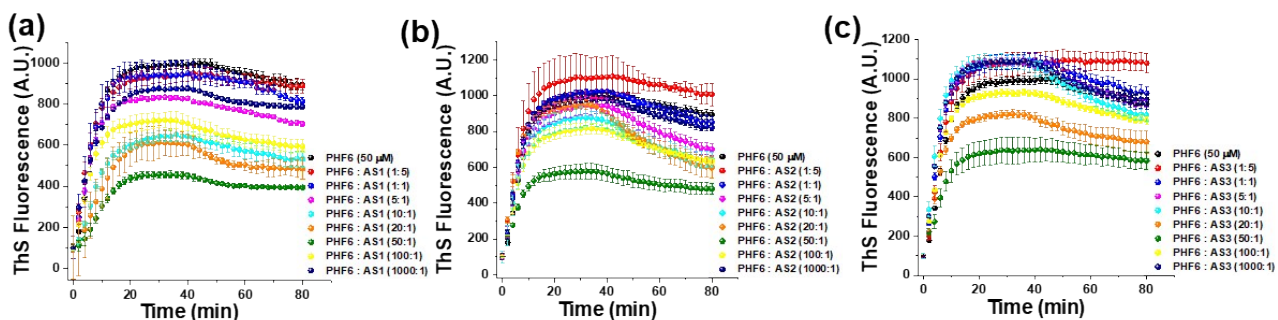


Figure S17. Time dependent ThS fluorescence of PHF6 aggregation ($50 \mu\text{M}$) in the absence or presence of various doses of conjugates (a) AS1, (b) AS2 and (c) AS3. Experiments were performed in MOPS (pH 7.2, 20 mM) at 25°C .

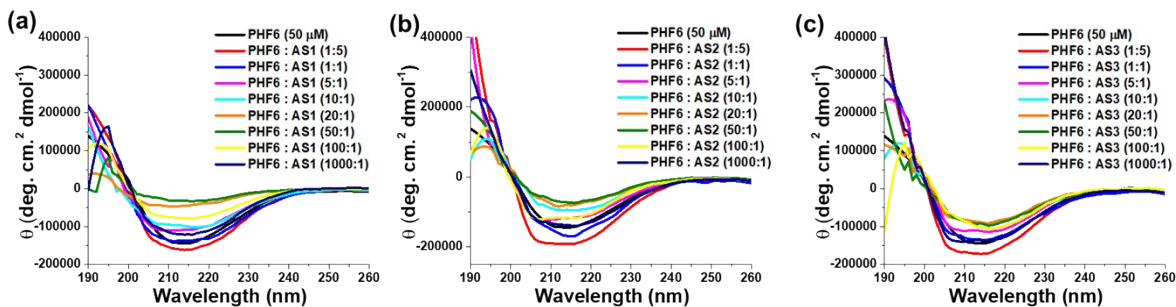


Figure S18. CD spectra for the inhibition of PHF6 aggregation ($50 \mu\text{M}$) in absence or presence of various doses (a) AS1, (b) AS2 and (c) AS3. Spectra were recorded after 60 min of PHF6 in absence or presence of the conjugates in MOPS (pH 7.2, 20 mM) at 25°C .

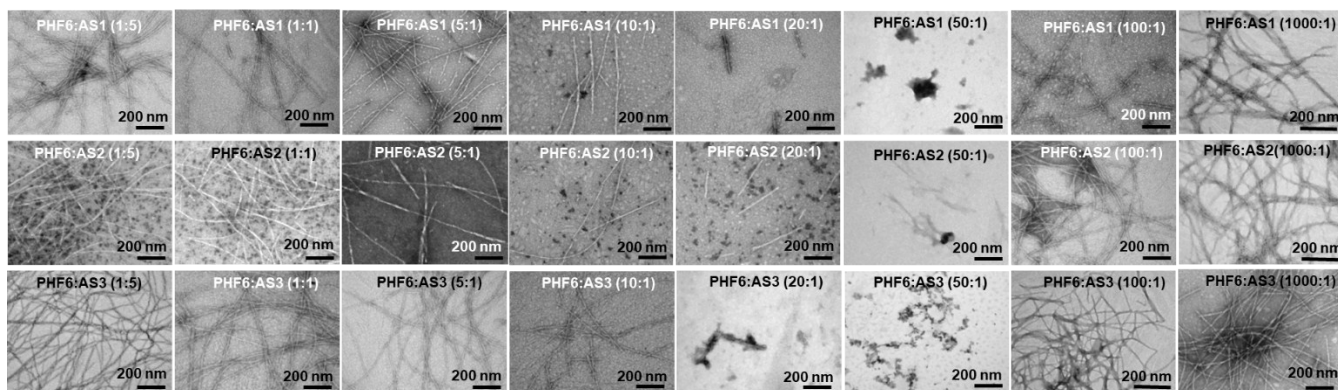


Figure S19. TEM images for the inhibition of PHF6 aggregation (50 μM) in the presence of various doses of AS1 (upper panel), AS2 (middle panel), and AS3 (lower panel). TEM grids were prepared immediately after end of the ThS experiment in MOPS (pH 7.2, 20 mM) at 25 $^{\circ}\text{C}$ and were kept under desiccator before capturing the images.

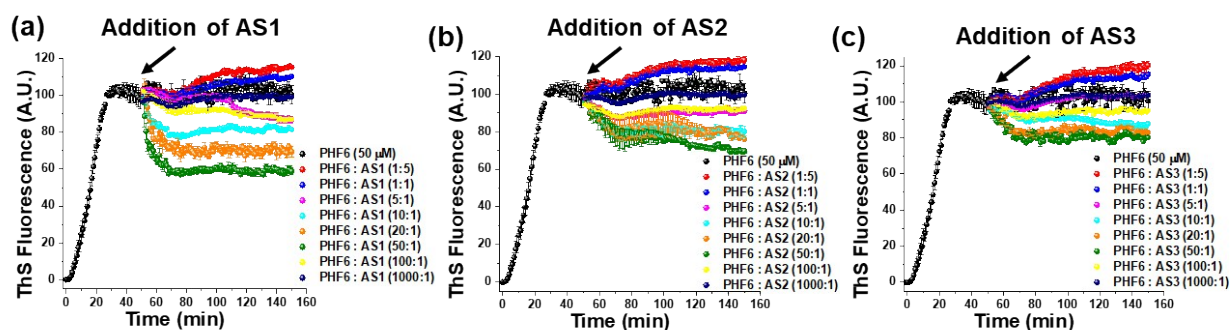


Figure S20. Time dependent ThS fluorescence for the disaggregation of preformed PHF6 fibrils (50 μM) in the absence or presence of different doses of the conjugate (a) AS1, (b) AS2 and (c) AS3. Experiments were performed in MOPS (pH 7.2, 20 mM) at 25 $^{\circ}\text{C}$.

CD results of untreated PFFs of PHF6 (black curve, Fig. 2g and Fig. S21†) showed a negative band at ~ 217 nm and a positive band at ~ 195 nm, reflecting β -sheet rich conformation. In the presence of the conjugates, CD intensity at ~ 217 nm declined as the doses of the conjugates decreased until 50:1-molar ratio, signifying disruption of the PFFs (Fig. S21†). However, at higher doses examined (PHF6:AS-1:5, 1:1), CD intensity at ~ 217 nm increased, indicating that the conjugates at these doses were incapable of

disassembling PFFs, in line with the ThS results. TEM analysis revealed that the untreated PHF6 displayed clear long dense fibrillar assemblies (Fig. 2h) as reported.^{5,6} The amount of fibrils was reduced with decreasing doses of the conjugates, until maximum reduction at 50:1 molar ratio of the conjugates (Fig. 2h and Fig. S22†). However, at the higher doses (PHF6:AS-1:5, 1:1) fibril density remained similar to that of the untreated fibril sample (Fig. S22†), suggesting that at the higher doses the conjugate were ineffective in disassembling of the PFFs.

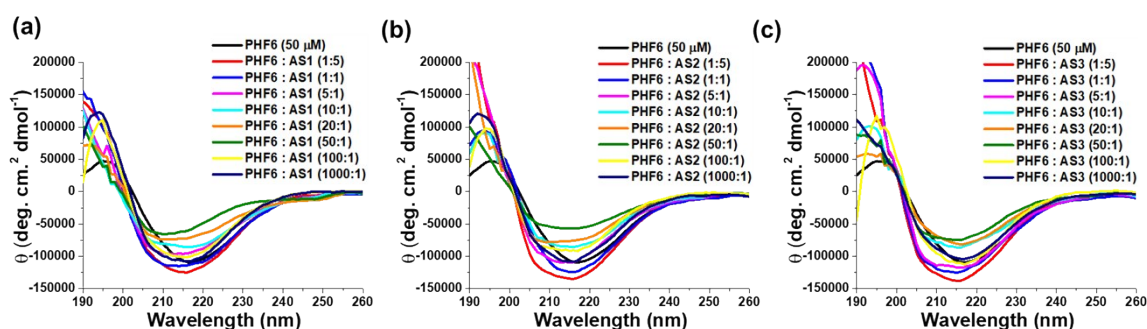


Figure S21. CD spectra for the disaggregation of preformed PHF6 fibrils (50 μM) in the absence or presence of various doses of (a) AS1, (b) AS2 and (c) AS3. Spectra were recorded after 150 min of total incubation of PHF6 in the absence or presence of the inhibitors in MOPS (pH 7.2, 20 mM) at 25 $^{\circ}\text{C}$.

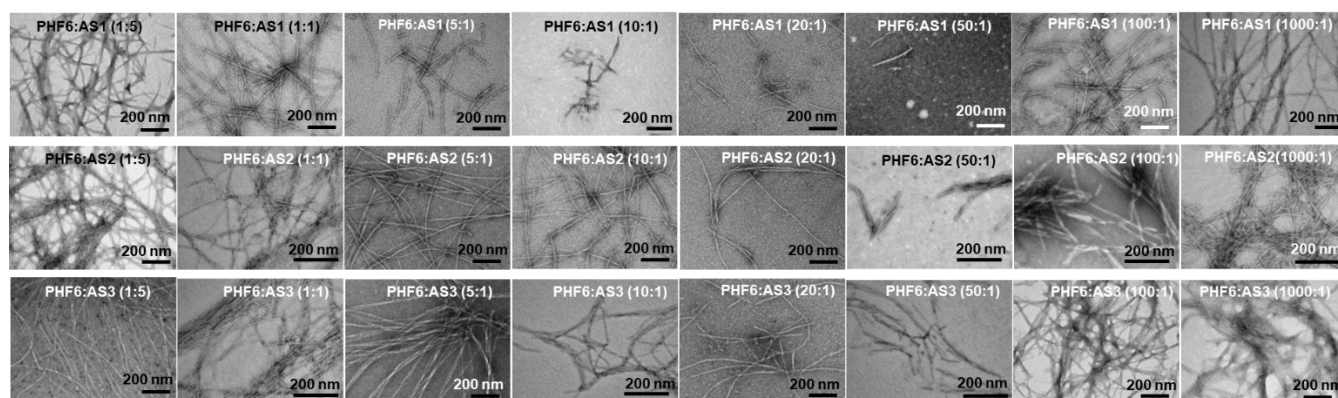


Figure S22. TEM images for the disaggregation of preformed PHF6 fibrils (50 μM) in presence of various doses of AS1 (upper panel), AS2 (middle panel), and AS3 (lower panel). TEM grids were prepared immediately after end of ThS experiment in MOPS (pH 7.2, 20 mM) at 25 $^{\circ}\text{C}$ and were kept under desiccator before capturing the images.

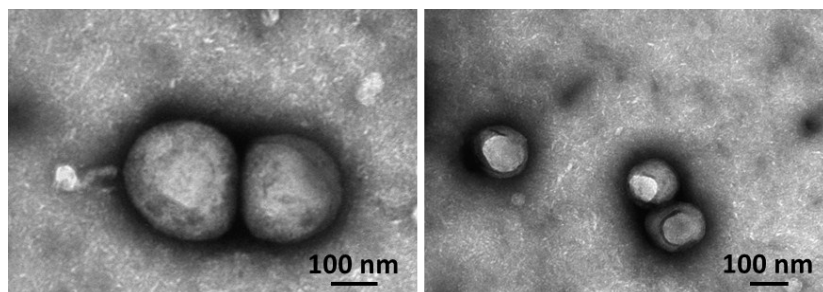


Figure S23. TEM images of LUVs at concentration of 20 μ M (stock concentration 2 mM) in MOPS (pH 7.2, 20 mM).

We next examined whether the conjugates disaggregated PHF6 fibrils into toxic or non-toxic species. As controls, PHF6 (50 μ M) was allowed to aggregate for 10 min and 150 min in the absence of the conjugates to generate oligomers and fibrils respectively, as inferred from ThS results (black curve, Fig. 2a). As experimental samples, conjugates were added to the 50 min aged PFFs of PHF6 (molar ratio PHF6: AS 50:1) and further incubated for 100 min. Then, LUVs were treated with the different samples. Spontaneous leakage from untreated LUVs was 6%; untreated PHF6 oligomers caused \sim 40% (red curve, Fig. S24d \dagger) and untreated mature fibrils caused \sim 17% leakage (blue curve, Fig. S24d \dagger), indicating that oligomers caused more damage to the LUVs than the matured fibrils.^{5,6} PFFs samples of PHF6 disaggregated by the conjugates caused less dye leakage \sim 11-17%. These results indicated that the conjugates disrupted PFFs of PHF6 into non-toxic species.

To verify whether the samples used for the LUV leakage assay contained oligomers or mature fibrils, both samples (aged 10 min and 150 min) were analysed under TEM and DLS. TEM micrographs showed that the 10 min aged PHF6 sample contained primarily smaller aggregates and some dispersed short fibrils were apparent (Fig. S25a \dagger). The 150 min aged PHF6 sample composed mainly of densely populated fibrils (Fig. S25b \dagger). DLS results indicate that the 10 min aged sample had a smaller hydrodynamic diameter (\sim 69 nm) than that of the 150 min aged sample (\sim 330 nm) (Fig. S26 \dagger). Collectively, TEM and DLS results indicate that the 10 min and 150 min aged PHF6 samples contained mostly oligomers and fibrils, respectively.

Cytotoxicity of the conjugates was examined by incubating them for 24h (0.2-250 μ M) with SH-SY5Y neuroblastoma cells (ATCC $\text{\textcircled{R}}$ CRL-2266) and evaluating cell viability by XTT (Biological Industries,

Israel) assay (Fig. S27†). At concentrations of 0.2-10 μM the conjugates displayed no cytotoxic effect (viability $\geq 95\%$). At higher concentrations (50-250 μM) cell viability was slightly reduced.

To examine the binding interaction between the AS molecules and PHF6, we performed Isothermal Titration Calorimetry (ITC) study. Freshly prepared monomeric PHF6 (400 μM) was titrated into a cell containing AS1 (70 μM) to measure the heat profile of the reaction. Results of the titration profile and the thermodynamic values were calculated and are displayed in Fig. S28† and Table S1†. Titration of PHF6 to AS1 resulted in exothermal peaks. Gibbs free energy (ΔG) was calculated from the enthalpy (ΔH) and entropy (ΔS) values to be negative (-30.1 kJ/mole), indicating that the reaction of PHF6 with AS1 was favourable and spontaneous at the experimental conditions used ($T=25\text{ }^\circ\text{C}$). The absolute value of ΔH (-91.09 kJ) was larger comparing to $T\Delta S$ (-60.3 kJ/mol), suggesting that the interaction between both molecules was enthalpy-driven. Electrostatic interactions and hydrogen bonding are reported to be the main factors affecting such an interaction. The relatively high value of the binding constant ($K_d = 4.14\text{ }\mu\text{M}$) supports the favourability of the interaction between PHF6 and the AS1. The stoichiometric ratio ($n=0.806$), quite close to 1, indicates that each AS1 molecule interacts separately with the peptide, suggesting that the interaction takes place with the monomers or lower order aggregates.

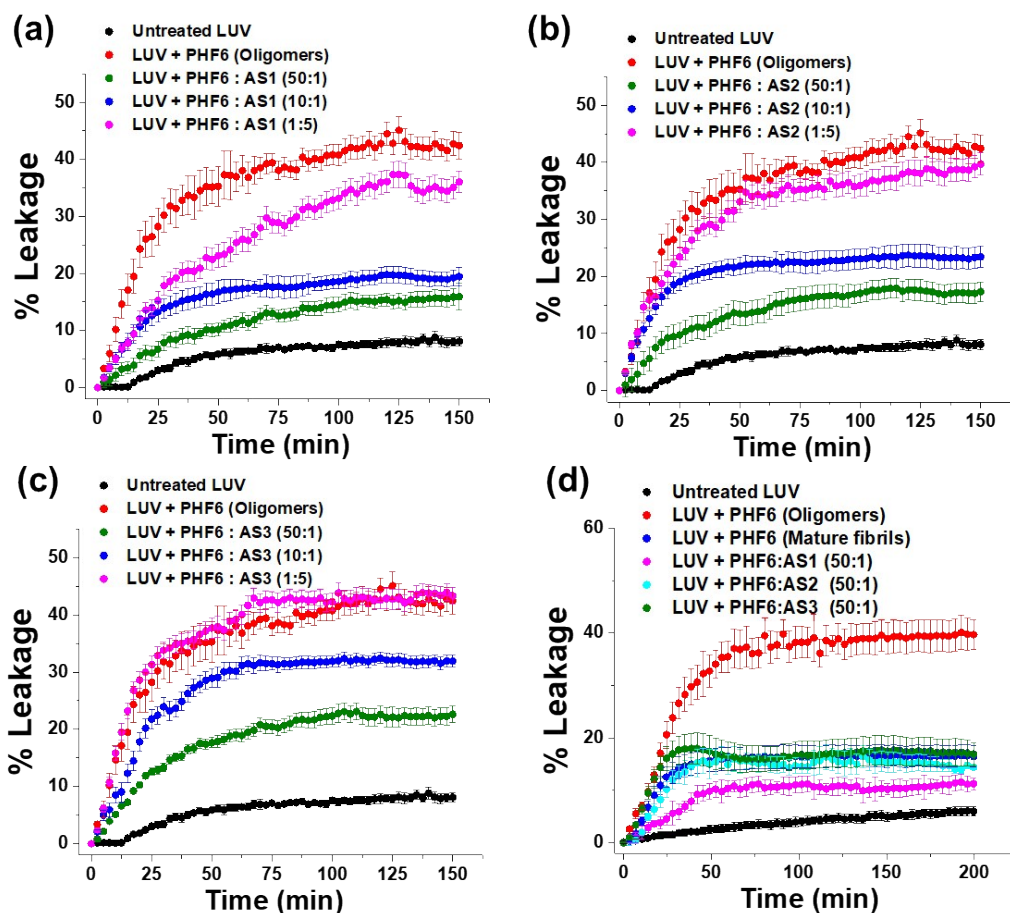


Figure S24. The effect of conjugate molecules on LUVs dye leakage caused by (a-c) PHF6 oligomers and (d) PHF6 mature fibrils, monitored by carboxyfluorescein dye emission. Spontaneous dye leakage from the LUVs is indicated as black curves.

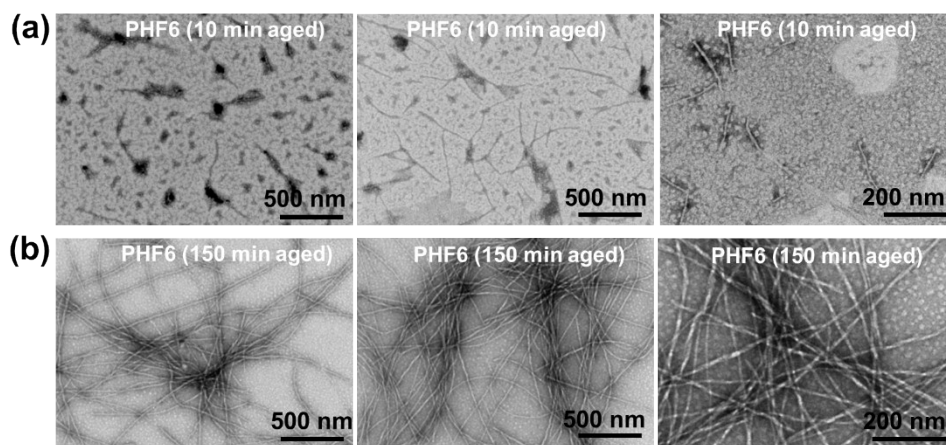


Figure S25. TEM images of PHF6 samples, incubated for (a) 10 min and (b) 150 min. TEM grids were prepared immediately at 10 min or 150 min of incubation in MOPS (pH 7.2, 20 mM) at 25 °C.

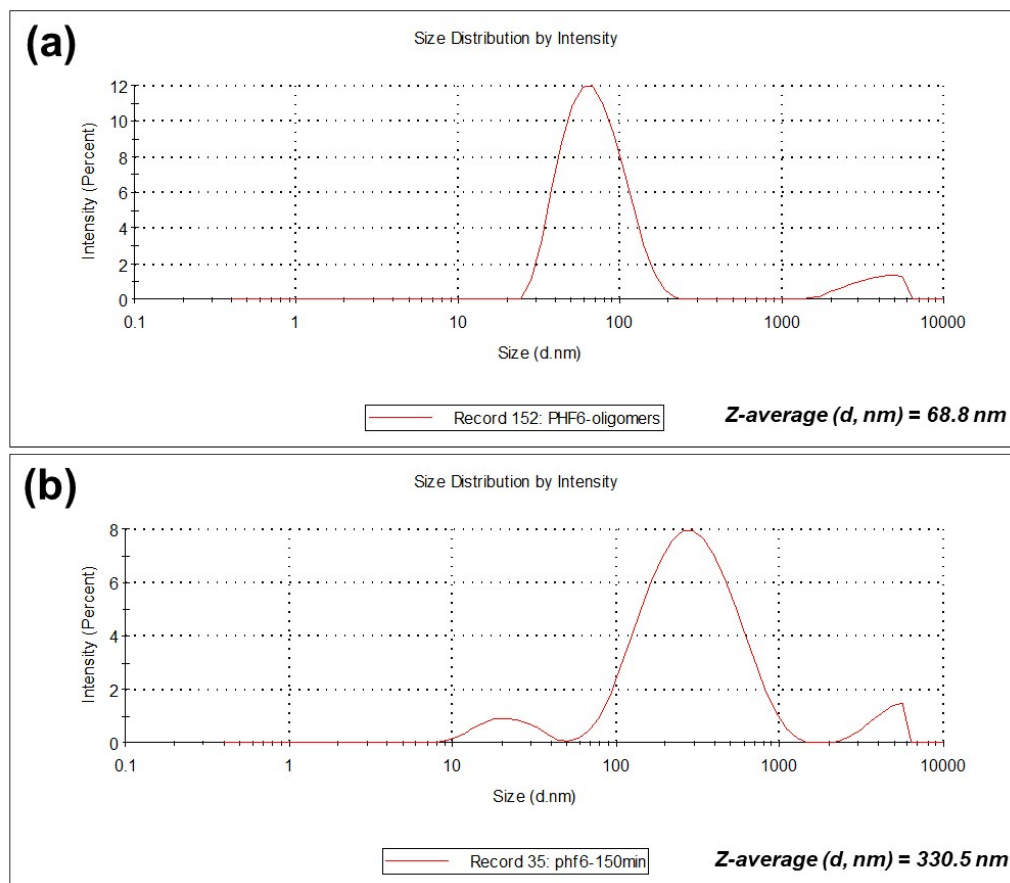


Figure S26. Size distribution curve observed in DLS measurement of PHF6 samples, incubated for (a) 10 min and (b) 150 min.

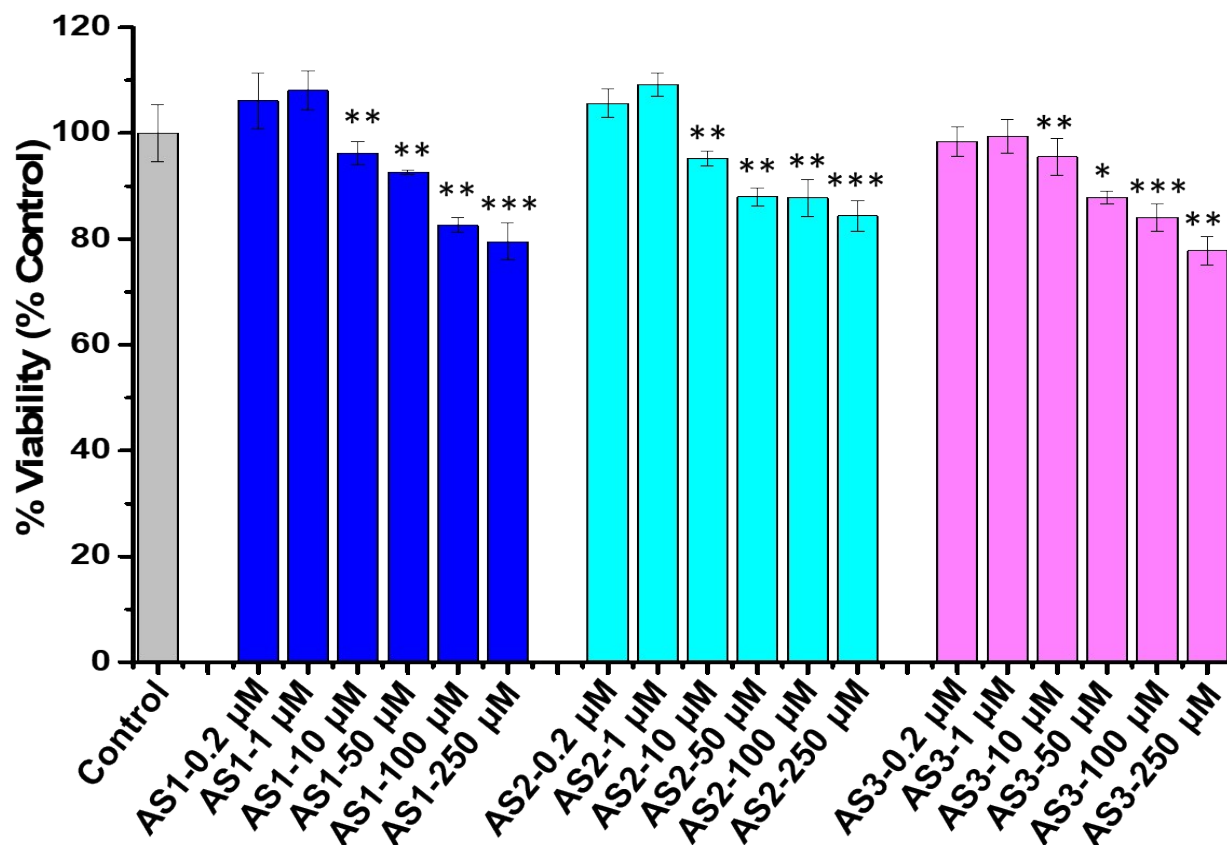


Figure S27. Cytotoxicity of the conjugate molecules towards SH-SY5Y cells. Cells were incubated with the conjugate molecules at various concentrations (0.2-250 μM) for 24 h and cell viability was evaluated by the XTT assay. Untreated cells were used as control and set to 100% viability. Results are average of 3 independent assays ($n = 3$ to 6, $\pm\text{SD}$) and are expressed as percentage of control cells. Significance (* $p < 0.05$), (** $p < 0.005$) and (***) $p < 0.001$).

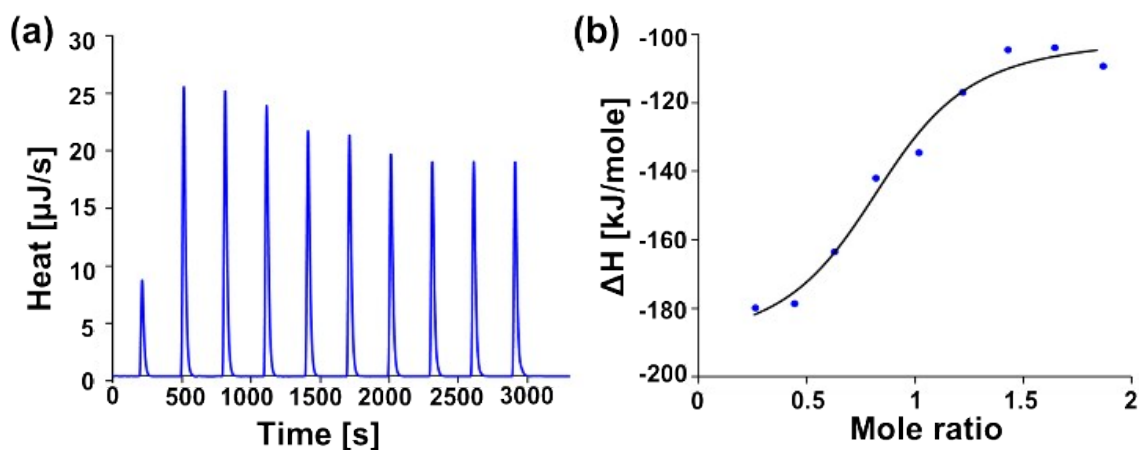


Figure S28. (a) Heat pattern during PHF6-AS1 binding measured by ITC. (b) Curve showing the enthalpy changes with increasing PHF6 to AS1 mole fraction.

Table S1. Thermodynamic properties of PHF6 and AS1 binding as determined by ITC measurements

Variable	Value	Confidence interval
Kd (M)	4.14 ⁻⁶	1.036*10 ⁻³
n	0.806	1.757
ΔH (kJ/mol)	-91.09	1147
ΔS (J/mol·K)	-202.5	N.A.

Since, AS1 displayed polar contacts with the residues of PHF6, we calculated the number of H-bonds formed by AS1 during the simulation. As shown in Fig. S29a†, each AS1 molecule formed ~two H-bonds with PHF6 peptides in the fibrillar arrangement. The number of main-chain H-bonds, known to maintain β-sheets in amyloids,^{6,13,14} between the peptides in the fibril in the absence or presence of AS1 were calculated over 20 ns. In the control system this number remained fairly constant throughout the simulation time, whereas the AS1-PHF6 system had less main-chain H-bonds even during the initial stages, and continued to remain lower than the control (Fig. S29b†), indicating that the presence of the conjugates disrupted these bonds, contributing to fibril disassembly.

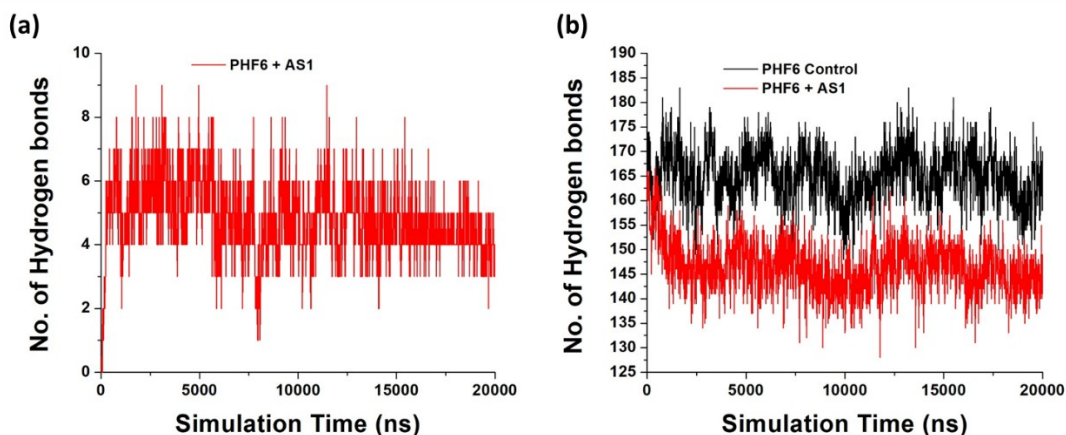


Figure S29. (a) Number of hydrogen bonds between AS1 and PHF6 peptides in the fibrillar arrangement (b) number of main-chain hydrogen bonds between the PHF6 peptides in the absence or presence of AS1.

We therefore examined whether the conjugates can self-aggregate by incubating each of them at the higher concentrations (100 μ M, 500 μ M and 1 mM) and monitoring their self-aggregation by ThS (Fig. S30†) and TEM (Fig. S31†). Both assays revealed that neither one of the conjugates self-aggregated at 100 μ M or 500 μ M whereas at higher concentrations (1 mM) slight aggregation was noticed, which was considerably lower (Fig. S30, S31†) than that of PHF6 (black curve, Fig. 2a) and it took much longer time to aggregate than PHF6 (1000 min vs. 50 min, respectively). These results support the above hypothesis regarding their effect at lower concentration as compared to higher concentration. We sought further support for the hypothesis by MD simulation of the PHF6 fibrils system in the presence of higher number (10 or 42) of AS1 molecules than describe above (Fig. 3). At the end of 20 ns (Fig. S32†), the higher number of AS1 conjugate molecules caused break to the fibril strand at only one location (Fig. S32b,d†), in contrast to the three breakages caused by three molecules of AS1 (Fig. 3g), which is concordant with our hypothesis.

We next examined whether the inverse correlation between the concentration of the AS conjugates and the degree of their effect on PHF6 aggregation is due to their constituent molecules tryptophan and glucosamine or is a unique property of the conjugate itself. ThS assay was performed to monitor the kinetics of PHF6 aggregation in the presence of AS1 or two control molecules, L-tryptophanamide (TrpNH₂) and methyl- α -D-glucopyranoside (MeGlu), at different doses (PHF6 : inhibitors = 1:5, 1:1, 20:1 and 50:1 molar ratio). The AS1 molecule was found to effectively inhibit aggregation of PHF6 at very low concentration (Fig. S33a,d†), whereas TrpNH₂ did not show any inhibitory effect (Fig. S33b,d†). However, we did observe that with increasing doses of MeGlu inhibition of PHF6 aggregation was enhanced (Fig. S33c,d†). Similar results were observed for the disaggregation of preformed PHF6 fibrils in the presence of these molecules (Fig. S34†). These results suggest that the intriguing inverse correlation of the effect of AS1 is independent of its constituent elements and represents a special feature of the conjugate itself. These findings imply that the inhibition and disaggregation effects of AS1 mainly arise from the glucopyranoside moiety.

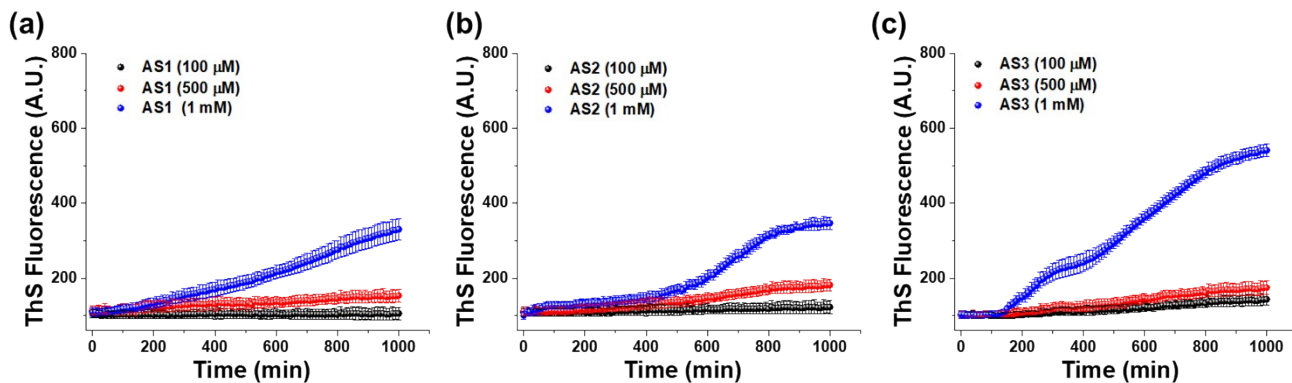


Figure S30. Time dependent ThS fluorescence of various concentrations of (a) AS1, (b) AS2 and (c) AS3. Experiments were performed in MOPS (pH 7.2, 20 mM) at 25 °C.

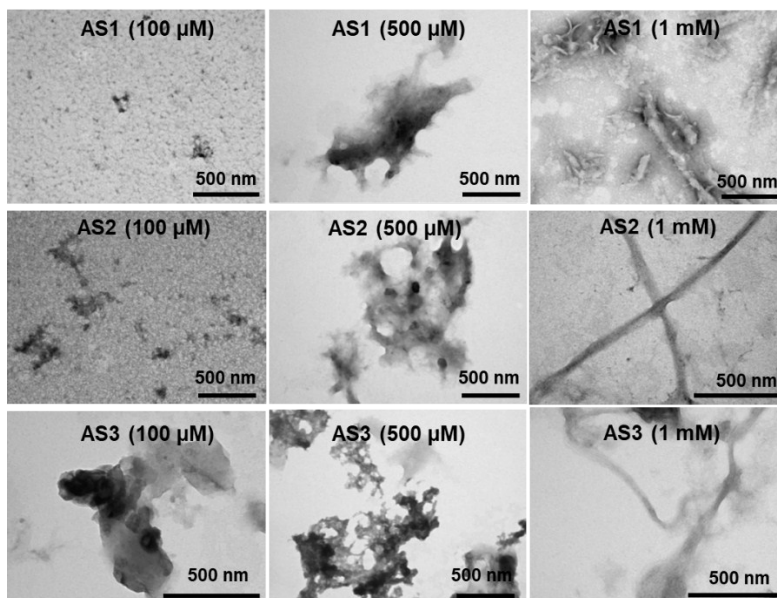


Figure S31. TEM images of various concentrations of AS1 (upper panel), (b) AS2 (middle panel), and (c) AS3 (lower panel). TEM grids were prepared immediately after the end of the ThS experiment in MOPS (pH 7.2, 20 mM) at 25 °C and were kept under desiccator before capturing the images.

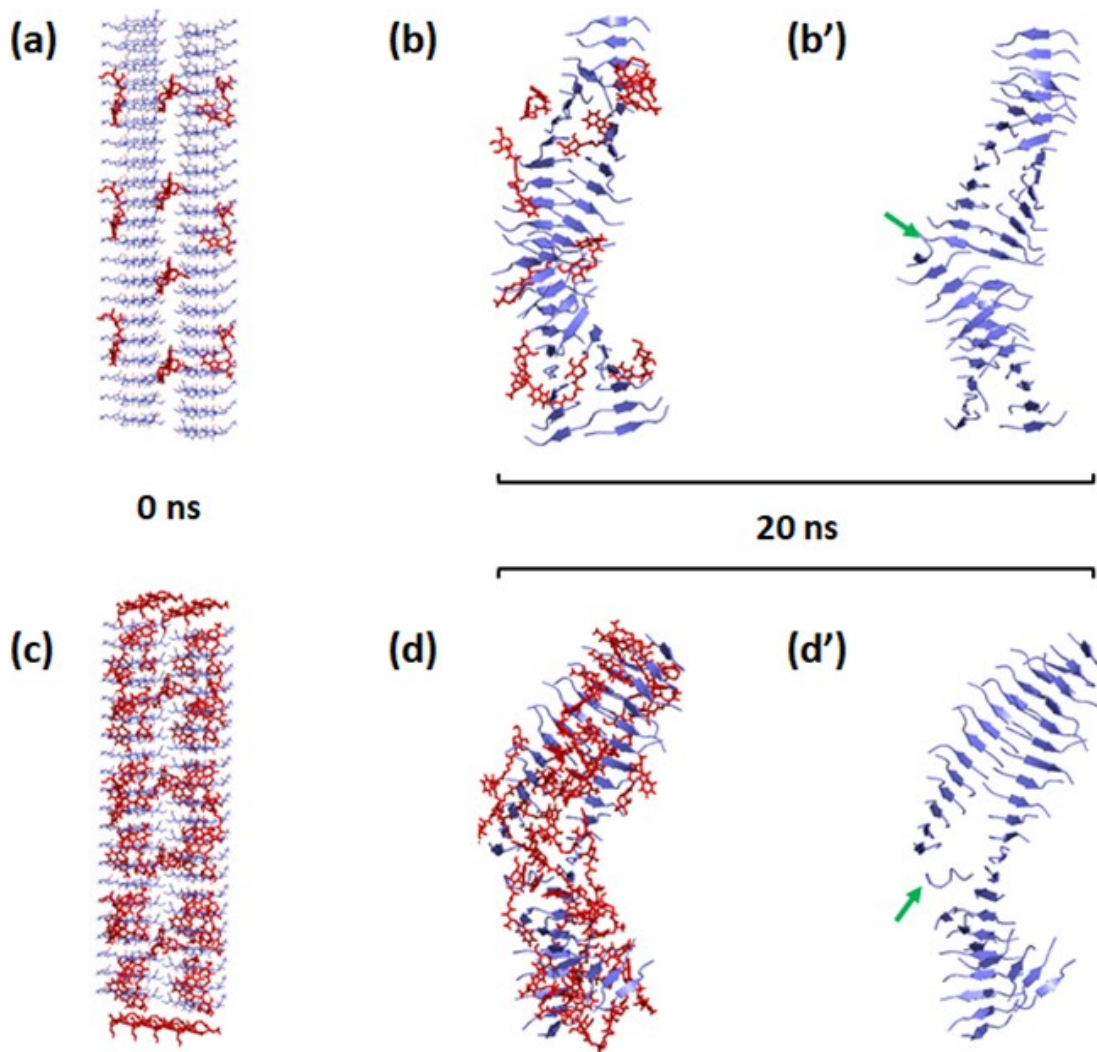


Figure S32. Trajectories of MD simulation of PHF6 fibril in the presence of (a) 10 molecules of AS1 at time 0, (b) at 20 ns and (c) 42 molecules of AS1 at time 0, (d) at 20 ns. (b') and (d') shows the breaks in fibrils at one location (the conjugate molecules are hidden). Break in fibril is indicated with green arrow.

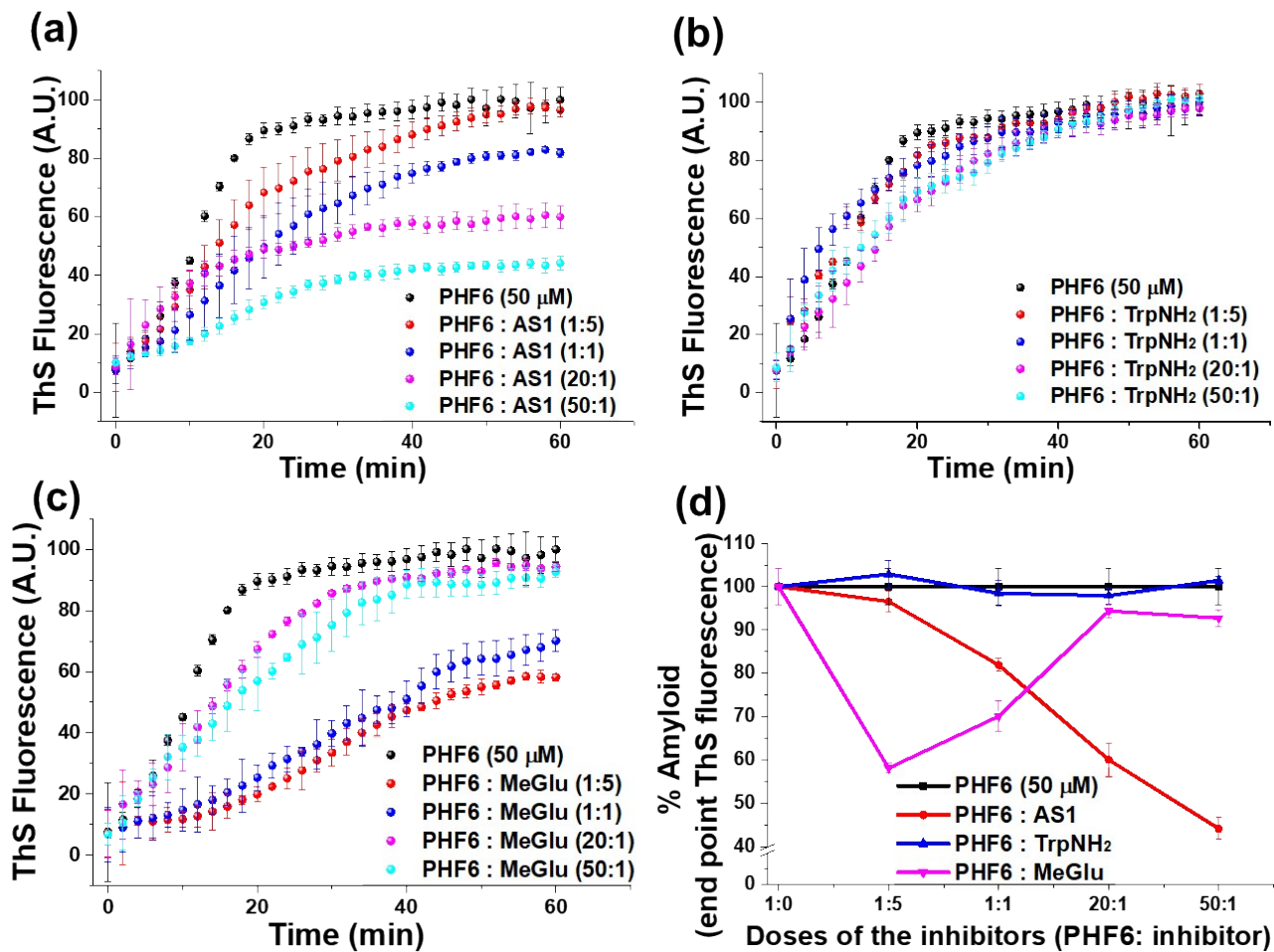


Figure S33. Time dependent ThS fluorescence of PHF6 aggregation (50 μM) in the absence or presence of various doses (PHF6 : conjugate- 1:5, 1:1, 20:1 and 50:1) of conjugates (a) AS1, (b) TrpNH₂ and (c) MeGlu. Experiments were performed in MOPS (pH 7.2, 20 mM) at 25 °C.

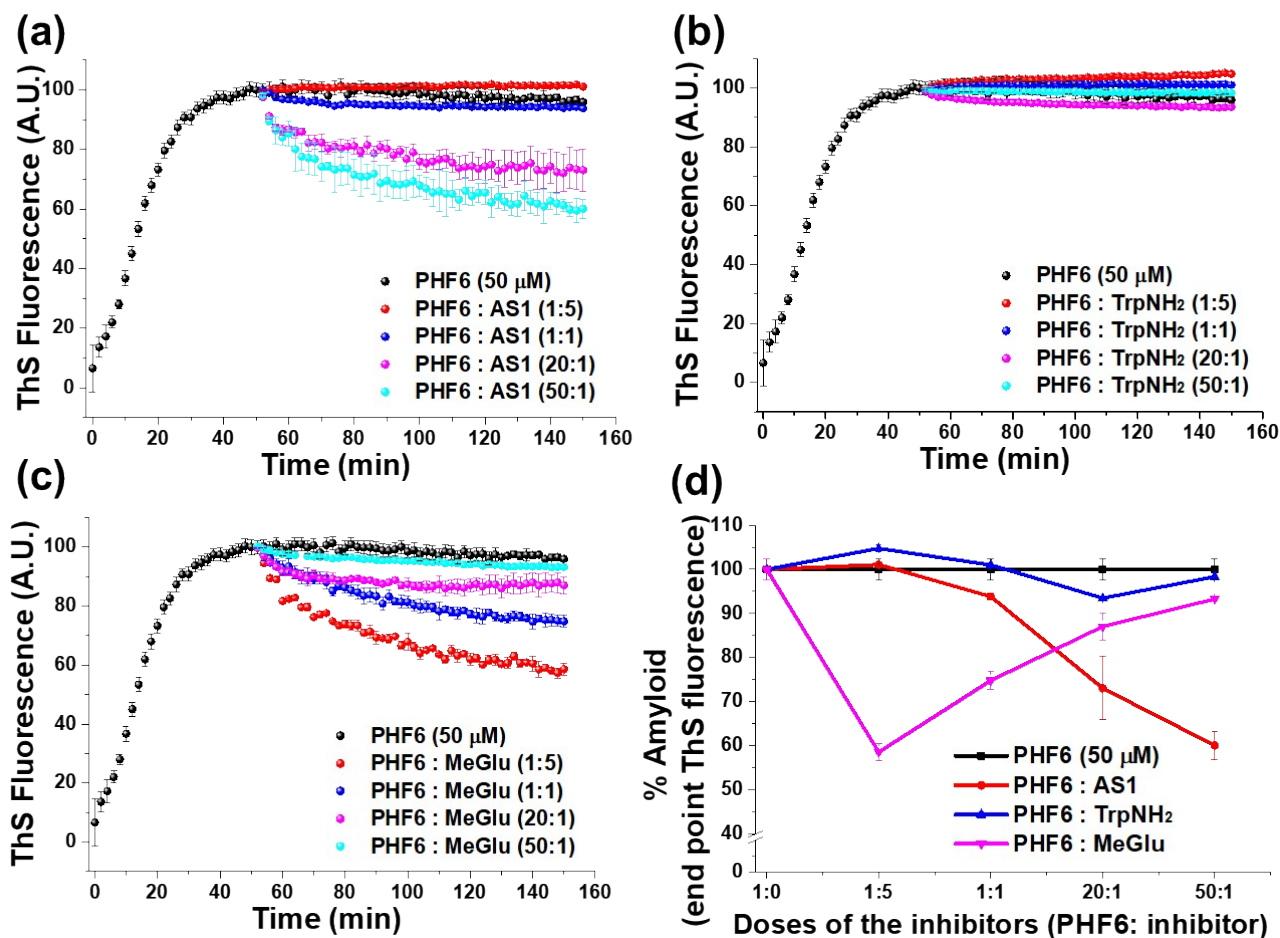


Figure S34. Time dependent ThS fluorescence for the disaggregation of preformed fibrils of PHF6 (50 μM) in the absence or presence of various doses (PHF6 : conjugate- 1:5, 1:1, 20:1 and 50:1) of conjugates (a) AS1, (b) TrpNH₂ and (c) MeGlu. Experiments were performed in MOPS (pH 7.2, 20 mM) at 25 °C.

References

- 1 N. N. Biswas, T. T. Yu, Ö. Kimyon, S. Nizalapur, C. R. Gardner, M. Manefield, R. Griffith, D. S. Black and N. Kumar, *Bioorg. Med. Chem.*, 2017, **25**, 1183–1194.
- 2 N. B. Shibin, R. Sreekanth, U. K. Aravind, K. M. Afsal Mohammed, N. V. Chandrashekar, J. Joseph, S. K. Sarkar, D. B. Naik and C. T. Aravindakumar, *J. Phys. Org. Chem.*, 2014, **27**, 478–483.
- 3 X. Zhu, J. Cai, J. Yang and Q. Su, *Carbohydr. Res.*, 2005, **340**, 1732–1738.

- 4 J. Lopez-Cervantes, D. I. Sonchez-Machado and K. E. Delgado-Rosas, *J. Chromatogr. Sci.*, 2007, **45**, 195–199.
- 5 A. Paul, G. K. Viswanathan, S. Mahapatra, G. Balboni, S. Pacifico, E. Gazit and D. Segal, *ACS Chem. Neurosci.*, 2019, **10**, 3510–3520.
- 6 V. G. KrishnaKumar, A. Paul, E. Gazit and D. Segal, *Sci. Rep.*, 2018, **8**, 71.
- 7 G. Malgieri, G. D’Abrosca, L. Pirone, A. Toto, M. Palmieri, L. Russo, M. F. M. Sciacca, R. Tatè, V. Sivo, I. Baglivo, R. Majewska, M. Coletta, P. V. Pedone, C. Isernia, M. De Stefano, S. Gianni, E. M. Pedone, D. Milardi and R. Fattorusso, *Chem. Sci.*, 2018, **9**, 3290–3298.
- 8 M. Konar, S. Bag, P. Roy and S. Dasgupta, *Int. J. Biol. Macromol.*, 2017, **103**, 1224–1231.
- 9 M. R. Sawaya, S. Sambashivan, R. Nelson, M. I. Ivanova, S. A. Sievers, M. I. Apostol, M. J. Thompson, M. Balbirnie, J. J. W. Wiltzius, H. T. McFarlane, A. O. Madsen, C. Riek and D. Eisenberg, *Nature*, 2007, **447**, 453–457.
- 10 N. Schmid, A. P. Eichenberger, A. Choutko, S. Riniker, M. Winger, A. E. Mark and W. F. van Gunsteren, *Eur. Biophys. J.*, 2011, **40**, 843–856.
- 11 E. Lindahl, B. Hess and D. van der Spoel, *Mol. Model. Annu.*, 2001, **7**, 306–317.
- 12 S. R. Gerben, J. A. Lemkul, A. M. Brown and D. R. Bevan, *J. Biomol. Struct. Dyn.*, 2014, **32**, 1817–1832.
- 13 F. X. Smit, J. A. Luiken and P. G. Bolhuis, *J. Phys. Chem. B*, 2017, **121**, 3250–3261.
- 14 M. von Bergen, P. Friedhoff, J. Biernat, J. Heberle, E. M. Mandelkow and E. Mandelkow, *Proc. Natl. Acad. Sci. U. S. A.*, 2000, **97**, 5129–5134.